ijecs open access www.ijecs.in
International Journal Of Engineering And Computer Science ISSN:2319-7242
Volume 3 Issue 9, September 2014 Page No. 8418-8438

Modeling and Control Solutions for Mechatronics Design of Solar Battery Electric Vehicles

Farhan A. Salem [1,3] **Ali *S.* Alosaimy**[2]
[1] Dept. of Mechanical Engineering, Mechatronics Engineering Prog., College of Engineering, Taif University, 888, Taif, Saudi Arabia.
[2] Dept. of Mechanical Engineering, Power Engineering Prog., College of Engineering, Taif University, 888, Taif, Saudi Arabia.
[3] Alpha center for Engineering Studies and Technology Researches, Amman, Jordan.
Email: salem_farh@yahoo.com

Abstract: In last years an increasing attention and more importance are dedicated to research in the fields of alternative vehicles, fuel consumption economy and reduction of related emissions. As an option to conventional vehicles, an increasing attention is being paid to the integration of Electric Vehicles (EV) and PhotoVoltaic (PV) panels resulting in Hybrid Solar Vehicle (HSV), and pure Solar Electric vehicle (SEV). This paper extends writers' previous works, and proposes a new generalized and refined model for Mechatronics design of pure Solar Electric Vehicles (SEV) and some considerations regarding design, modeling and control solutions. The proposed SEV system model consists of eight main subsystems, each subsystem, is mathematically described and corresponding Simulink sub-model is developed, then an integrated generalized model of all subsystems is developed and tested. The proposed SEV system model is developed to help in facing challenges in developing Mechatronics SEV systems, in particular; early identifying system level problems and ensuring that all design requirements are met, as well as, for research purposes and application in educational process. Model is developed to allow designer to have the maximum output data to to design, tested and evaluate overall SEV system and/or each subsystem outputs characteristics and response, for desired overall and/or either subsystem's specific outputs, under various PV subsystem input operating conditions, to meet particular SEV system requirements and performance.The obtained results show the simplicity, accuracy and applicability of the presented models to help in Mechatronics design of SEV system .

Keywords: Mechatronics, Electric vehicle (EV), Solar Electric vehicle (SEV), PV Panel, Modeling/Simulation.

[1] Introduction

Modeling, simulation, analysis and evaluation processes in Mechatronics design consists of two levels; sub-systems models and whole system model with various sub-system models interacting similar to real situation, the subsystems models and the whole system model, are to be tested and analyzed for desired system requirements and performance [1].
With the growing requirements to improve fuel consumption economy and reduce related emissions, as an option to conventional vehicles, Electric Vehicles (EVs), represent a good and feasible solution, particularly, in case of intermittent use in urban areas.
The EV was invented around middle of 19th century, now EV can include electric cars, electric trains, electric airplanes, electric boats, electric motorcycles, golf cars, go-karts and scooters even electric spacecraft. The EV system consists of the next major subsystems, shown in Figure 1; an electric machine subsystem (one or more electric or traction motors) for propulsion drive system, the vehicle subsystem, electrical energy source, control subsystems as a central control, and power converter subsystem as a device that converts electrical energy source with variable needs of the electric vehicle by switching devices [1-2].
Meanwhile EV generally use a battery as its main energy source [3-5] the batteries on electric vehicles have a weakness that has the capacity and service life is limited, Several new battery types have been developed to deliver more power with reduced weight. Based on how and where the electricity is produced, an EV can be separated into the following three major groups [1]; (1) *Powered from an external power station*, e.g. Trolleybuses. (2*) Powered by an on-board electrical generator* such as an internal combustion engine (a hybrid electric vehicle HEV) or a hydrogen fuel cell (see Figure 1(a)). HEV are dual-fuel vehicles in which both the electric motor and internal combustion engine can drive the wheels, where depending on the vehicle size and construction, the electric motor accelerates the vehicle to about 60-80 K/h, and then the internal combustion engine takes over. The battery is recharged by the gasoline engine and regenerative braking, where regenerative braking converts kinetic energy that otherwise would be lost as heat in the brake pads into electricity to charge the battery, the Ford Fusion Hybrid and Toyota *Prius* are examples of this type of hybrid [6]. As an extension of hybrid vehicle technology, *Plug-In Hybrid Electric Vehicles* (PHEV) are developed (shown Figure 2), the main difference is the larger capacity and differently designed battery pack that can be recharged from the electricity grid [7] at home, by the gasoline engine and regenerative braking. PHEV retains all the functionality of HEV but with higher than conventional mileage and lower emissions. (3) *Powered by stored electricity from an off-board generation system* e.g. Battery Electric Vehicles (BEV) shown in Figure 3, there is no gasoline engine, all the power needs are supplied 100% by the battery electricity, which is recharged from the electricity grid and do not require trips to the gas station. The battery has greater capacity because it has to provide all the range and power needed for acceleration and accessories such as clocks, security

systems, automatic diagnostic systems, vent fans, ignition systems, entertainment systems, air conditioning, heating, etc. Battery Electric Vehicles (BEV) are like other vehicles, they are practical for everyday use, with the same safety standards and enough space for passengers and cargo, but differ in that they are highly efficient, very smart and accelerate quickly and very quietly, some can reach speeds over 150 Km/h. In addition to these groups, a fourth group exist that can fall under BEV, and can be called *Small Electric Vehicles* (SmEV), three- and four-wheel Vehicles with maximum speeds of 45 Km/h, examples include go-caret, golf carts, global electric motorcars and Chrysler subsidiary, golf carts dominate this group.

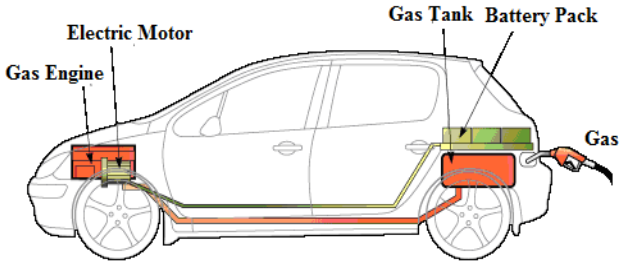

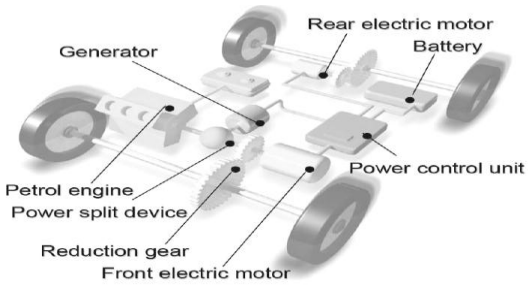

Figure 1 (a) Dual-fuel-Hybrid electric vehicle HEV [7]

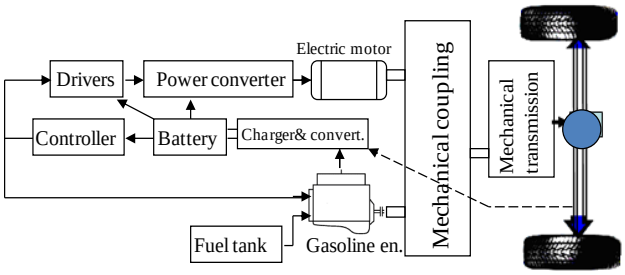

Figure 1(b) Architecture of *(Parallel)* Hybrid Electric Vehicles (HEV)

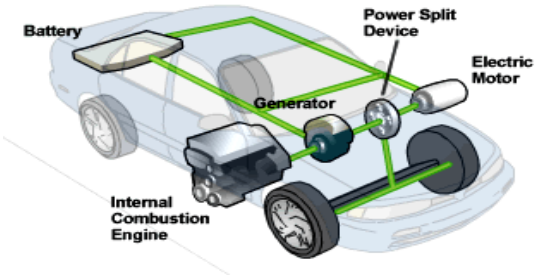

Figure 1(c) source: http://www. fueleconomy.gov/feg/hybridtech. shtml

Figure 1(a)(b)(c) Hybrid Electric Vehicles (HEV) and architecture, it combines an internal combustion engine and an electric motor.

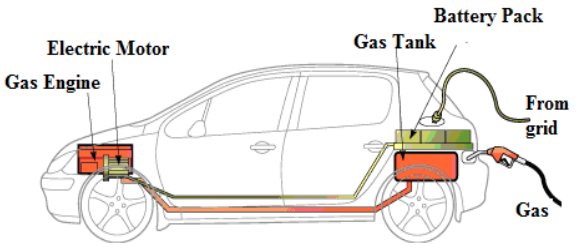

Figure 2 (a) Plug-In Hybrid Electric Vehicle (PHEV)[7]

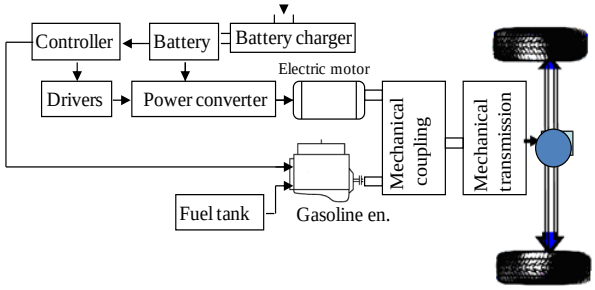

Figure 2(b) Architecture Plug-In Hybrid Electric Vehicles (PHEV)[1]

Figure 2 (a)(b) Plug-In Hybrid Electric Vehicle and architecture

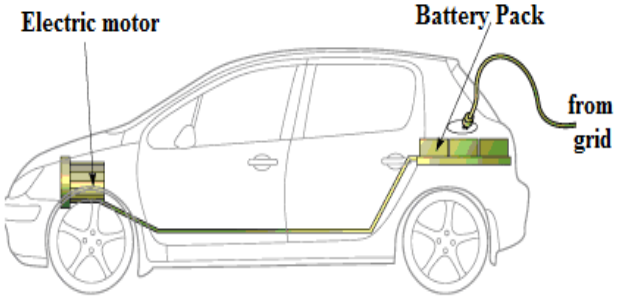

Figure 3(a) Battery Electric Vehicle (BEV)[7]

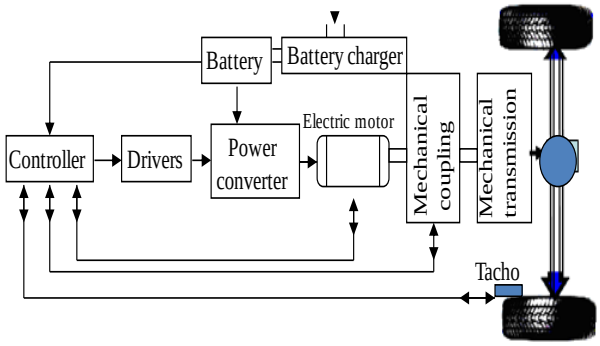

Fig. 2(b) Architecture of Battery Electric Vehicles (BEV)[1]

Figure 3(a)(b) Battery Electric Vehicle and Architecture

1.1 Hybrid Solar Electric Vehicle (HSEV)

In last years an increasing attention is being paid to the integration of EV and PhotoVoltaic (PV) panels, due to the fact that Solar energy, is a kind of free, gratis, abundant, renewable and largely diffuse energy, and due to the decreasing cost and increasing efficiency of PV panels and the growing requirements to improve fuel consumption economy and reduce related emissions [8-9], as confirmed by the recent launch of a HEV mounting solar panels by a major automotive company. The combination of these two elements born the idea of Hybrid Solar Electric Vehicles (HSEV). Based on this, Solar Electric Vehicle (SEV) can be defined as a modified version of *Battery Electric Vehicles* (BEV), it is an automotive electric vehicle driven by electric energy obtained as a result of photovoltaic conversion (uses the PV panel as electricity generator to convert the irradiance from sunlight into electricity using photovoltaic system) to generate its own power for propulsion and for storing in batteries, it is *lightweight* and *aerodynamically* efficient [10-16], all the power needs are supplied 100% by the PV panel subsystem.

In spite of their potential interest, HSEV (e.g. cars) have received relatively little attention in literature [10], where, Solar Vehicle prototypes have been built and tested, mainly for racing and demonstrative purposes [11-13] and for didactic aims and prototype competitions. An innovative prototype has been developed at western Washington University [14-15] in the 90s, adopting advanced solutions for materials, aerodynamic drag reduction and PV power maximization with peak power tracking. Other studies and prototypes on solar hybrid vehicles have been presented by Japanese researchers [16-17] and at the Queensland University [18]. Despite a significant technological effort and some spectacular outcomes, several limitations, such as low power density, unpredictable availability of solar source and energetic drawbacks (i.e. increase in weight, friction and aerodynamic losses due to additional components), cause *pure* Solar Electric Vehicles (e.g. cars) to be still far from practical feasibility. On the other hand, the concept of a hybrid electric car assisted by solar panels appears more realistic [10][14-16]. In fact, due to relevant research efforts [11,24] in the last decades *Hybrid Electric Vehicles* (HEV) have evolved to industrial maturity. These vehicles now represent a realistic solution to important issues, such as the reduction of gaseous pollution in urban conditions drive as well as the energy saving requirements. Moreover, there are a large number of drivers utilizing daily their car, for short trips and with limited power demand. Some recent studies, conducted by the UK government, report that about 71 % of UK users reach their office by car, and 46 % of them have trips shorter than 20 minutes, mostly with only one passenger (i.e. the driver) [19]. The above considerations open promising perspectives with regard to the integration of solar panels with EV, with particular interest in the opportunity of storing energy even during parking phases [11].

Most of relatively little pure SEV researches in literature [2-18] concerned with separate specific system or subsystem design, dynamics analysis, control or application. To help in facing the two top challenges in developing Mechatronics pure SEV systems, particularly; early identifying system level problems and ensuring that all design requirements are met, a generalized and refined model of pure SEV system is of concern. This paper extends writer's previous works [20-31] and proposes a new generalized and refined model for Mechatronics design of a pure SEV system (battery electric vehicle assisted by solar panels) and some considerations regarding design, modeling and control solutions. The proposed model can be applied in selecting, designing, testing and evaluation processes of Battery SEV applications including; solar electric cars, solar electric trains, solar electric boats, and solar electric motorcycles, solar golf cars, go-karts and solar scooters.

1.2 System description

The SEV system in the form of the proposed generalized BSEV system model, considering above application examples, in its simplified form, can be considered consisting of three major subsystems: the PV subsystem, the vehicle subsystem and DC machine subsystem, in particular, BSEV system can be considered consisting of the next main eight major components shown in Figure 4; PV panel , DC/DC converter , PWM generator, battery bank, DC machine (one or more electric or traction motors) for propulsion drive system, sensing devices, control units (one or more controllers) and vehicle platform with its kinematic and dynamic model. this paper is organized into corresponding parts, where each subsystem, is to be mathematically described and corresponding Simulink sub-model is to be developed, then an integrated generalized model of all subsystems is to be developed, the sub-models and whole system model, are to be developed to allow designer to have the maximum output data to select, integrate, control and evaluate the whole HSEV system and/or each subsystem output characteristics and response, for desired overall and/or either subsystem's specific outputs, under various PV subsystem input operating conditions, to meet particular HSEV system requirements and performance, The proposed BSEV system and the block diagram representation are shown in Figure 4 (a)(b).

1.3 SEV design, advantages and limitations [10][32-23]

For pure SEV, the series structure shown in Figure 4, is prevailing, due its simpler structure and to the possibility of integration with grid. Moreover, the adoption of electric motors integrated into the wheels, would allow to reduce mechanical losses and to apply advanced traction control strategies.

The proper design and optimization of the whole SEV, including powertrain system, sizing, shape, dimension, performance, weight and costs, will maximize the benefits resulting from the integration of Photovoltaic with Battery EV, and allow meeting a significant share of the total energy required with the energy captured by the panels, during both driving and parking phases [30]. In designing SEV, particular attention has to be paid in maximizing the net power from solar panels, and in energy management and control, also, to include battery with highly efficient and capacity (li-ion, lipolymer, zinc-air), of 80 – 95 % and be characterized with low mass, low value of the rolling resistance coefficient, and aerodynamic shape. *Energy density* is the main limitation of integrating PV in vehicle industry, the power generated by mounted on fixed location on vehicle' roof solar panel, that depends on it's type, efficiency and size (area that can be exposed to sunlight), mainly is less than the maximum required power of vehicle, that depends on vehicle's size, weight, electric accessories and road-load disturbances. But benefits of integrating PV can be maximized when SEV are used, in case of intermittent use in urban areas spending most of their time parked outdoor, and in countries where high solar radiation. *Vehicle weight;* the parametric weight model of the SEV can be obtained adding the weight of the specific components (e.g.

PV panels, battery pack, Electric Motor, Inverter) to the weight of the conventional vehicle equipped with ICE and by subtracting the contribution of the components resized or not present in the HSV (i.e. ICE, gearbox, clutch [17]. *Controlling the performance of SEV* is not a simple task, where the design and operation parameters of SEV, as well as the road condition are always varying, generally, SEV must to be designed and controlled to maximize the net power from solar panels, consume minimum electric power, while maintaining main characteristics of efficiency in driving the distance using the least amount of energy, quick, quiet motion and acceleration (smooth driving for comfortable riding). Therefore, it is recommended to include vehicle and PV subsystems currents and speed controllers, the speed controller should be designed to make the system robust, adaptive and improving the system on both dynamic and steady state performances (fast responsive and low-ripple)[1].The following are the main *advantages* of integrating PV in automotive;(1) Due the worldwide demand for personal mobility is rapidly growing, the integration of solar energy, improves the growing requirements to improve fuel consumption economy and reduce acoustic and atmospheric pollution emissions.(2) The use of free, gratis, abundant, renewable and largely diffuse solar energy.(3) Adding PV cells to a HEV allows reducing the generator and internal combustion engine sizes leading to a reduction of the operation costs. (4) HSEV is equipped with a number of devices fed by batteries that provide all the range and power needed for acceleration and accessories, a PV source installed on EV, is able to directly provide the excess energy to the battery preserving its charge level and extending its life, also feed electric accessories.

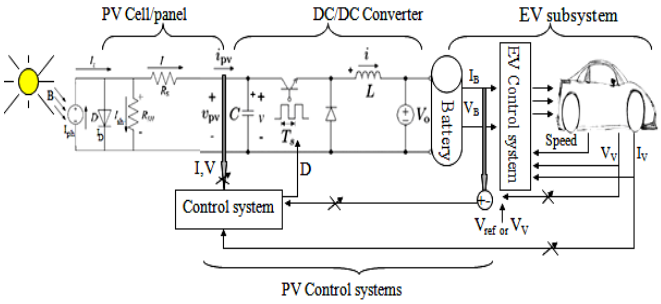

Figure 4 (a) SEV system circuit diagram, main components and control

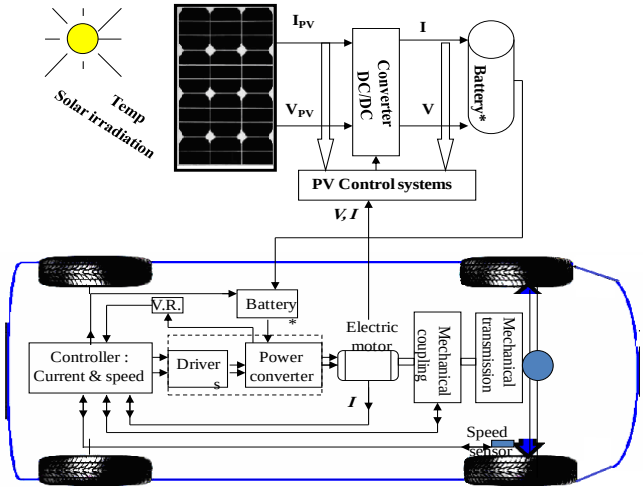

Figure 4(b) SEV system diagram, components and control
Figure 4(a)(b) SEV system diagram and main subsystems, including; PV panel, DC/DC converter, battery bank, DC machine, control units and platform.

2. SEV system modeling

In the following, each subsystem of SEV eight subsystems, is to be described mathematically and corresponding Simulink sub-model is to be developed, then all sub-models are to be integrated to developed one generalized SEV system model.

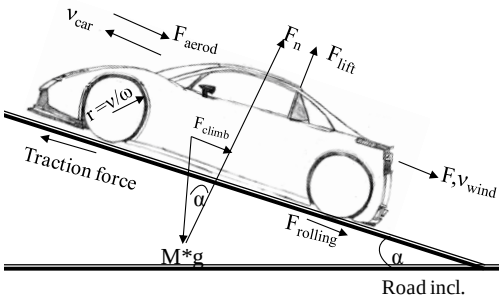

Figure 5(a)

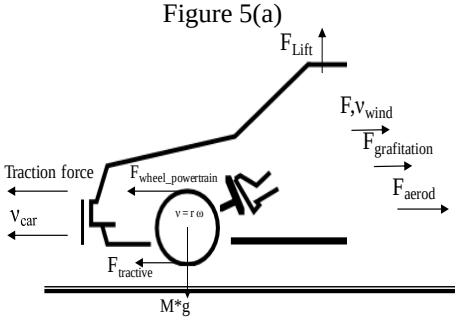

Figure 5(b)

Figure 5(a)(b) Forces acting on a vehicle moving vehicle

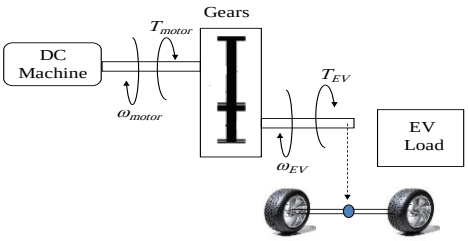

Figure 6 EV's Electromechanical structure

2.1 Modeling and design of PV Panel-Converter subsystem

SEV uses the PV panel as electricity generator to convert the irradiance from sunlight into electricity to generate its own power for propulsion and for storing in batteries, also uses power converter as a device that converts electrical energy source with variable needs of the electric vehicle by switching devices. The PV Panel-Converter (PVPC) system consists of three main subsystems; PV panel, DC/DC buck converter and battery pack subsystems.

The circuit diagram of PV cell is shown as sub-circuit in Figure 4(a). A mathematical description of a PV cell/panel in terms of output voltage, current, power and I-V and P-V characteristics has been studied for the past four decades and can be found in different resources, many of which are listed in [24]. ***The output net current of PV cell I***, and the V-I characteristic equation of a PV cell are given by Eq.(1), it is the difference of three currents; the light-generated *photocurrent* I_{ph}, *diode* current I_d and the *shunt* current I_{RSH} . The output voltage, current and power of PV array vary as functions of solar irradiation level β, temperature T , cell voltage V and load current I. The PV panel model and mask is shown as sub-model of the generalized SEV system model shown in Figure

10(e). the cell's saturation current (*Is*) varies with the cell temperature, which is described as by(33).

Running PV panel simulink sub-model, for PV parameters defined in Table 1, at standard operating conditions of irradiation $\beta=1000$, and temperature $T=25$, will result in P-V and I-V characteristics shown in Fig. 7(a)(b) and can be shown as visual numerical values of cell's-panels current, voltage, powers, efficiency and fill factor, these curves show that, this is 3.926 Watt PV cell with $I_{SC} = 8.13\ A$, $Vo= 0.6120V$, $I_{max} =7.852\ A$, $V_{max} =0.5\ V$, $(MPP = I_{max} * V_{max} =7.852 *0.5=3.926)$.

Power converters can be classified intro three main types; step-up, step-down and step up and down. Most used and simple to model include *Boost, Buck and buck-boost converters* [21-22]. In this paper step-down DC/DC *Buck converter*s is used, the circuit diagram of Buck converter is shown as sub-circuit in Figure 4(a). In [23], different models of *Buck* converter are derived, developed in Simulink and tested. The *Buck converter* model and mask are shown as sub-model of the generalized SEV system model shown in Figure 10(f).

Duty cycle is the ratio of output voltage to input voltage is given by Eq.(2), and defined as the ratio of the ON time of the Buck converter switch to the total switching period, where: I_{out} and I_{in}, : the output and input currents. ***The PWM generator*** is assumed as ideal gain system, the duty cycle of the PWM output will be multiplied with gain $Kv= K_D$

In [20-23] PVPC system generalized model is developed in Simulink and tested, by integration both PV panel and buck converter sub-models resulting in generalized PVPC sub-model and mask shown as sub-model of the generalized SEV system model in Figure 10(f,h,he), this generalized PVPC model is designed to allow designer to have maximum numerical visual and graphical data to select, design and analyze a given both PV and converter subsystems for desired output performance and characteristics under given operation condition, including; cell's-panels current, voltage, powers, efficiency fill factor, converter's output voltage and current.

$$I = I_{ph} - I_d - \mathrm{I}_{RSH}$$

$$\mathrm{I} = \left[\left(I_{sc} + K_i \left(T - T_{ref} \right) \right) \frac{\beta}{1000} \right] - \left[\mathrm{I}_s \left(e^{\frac{q(V+IR_S)}{NKT}} - 1 \right) \right] - \left[\frac{V + R_S I}{R_{sh}} \right] \quad (1)$$

$$I_S(T) = I_S \left[\frac{T}{T_{ref}} \right]^3 e^{\left[\left(\frac{T}{T_{ref}} - 1 \right) \frac{qE_g}{NKT} \right]} \Leftrightarrow I_S(T) = I_S \left[\frac{T}{T_{ref}} \right]^3 e^{\left[\left(\frac{1}{T_{ref}} - \frac{1}{T} \right) \frac{qE_g}{NKT} \right]}$$

$$\frac{V_{out}}{V_{in}} = D = \frac{I_{in}}{I_{out}} \Rightarrow V_{out} = D * V_{in} \Leftrightarrow D = \frac{T_{on}}{T_{on} + T_{off}} \quad (2)$$

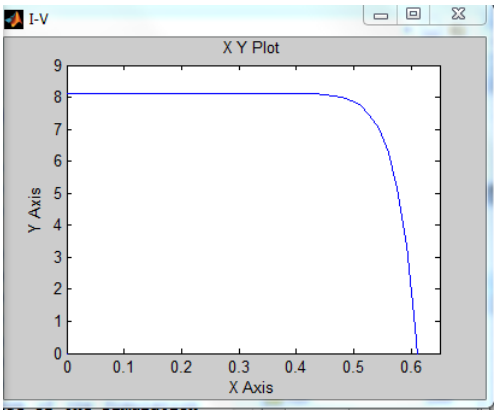

Fig. 7 (a) V-I Characteristics for β=1000, and T=25

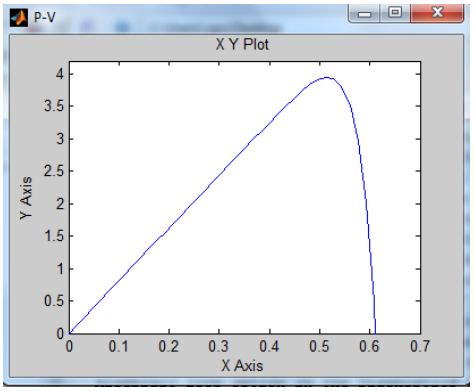

Fig. 5 (b) P-V Characteristics for β=1000, and T=25

2.4 Modeling Vehicle-platform dynamics

The electromechanical structure of EV is shown in Figure 6. The motor torque is proportional to the wheel radius, *r* and the force acting on it. When deriving an accurate mathematical model for a given vehicle including EVs, it is important to study and analyze dynamics between the road, wheel and EV considering all the forces applied upon the EV system. The modeling of an EV system dynamics involves the balance among the several acting on a running EV forces, these acting forces are categorized into road-load and tractive force. The road-load force consists of the gravitational force, hill-climbing force, rolling resistance of the tires, the aerodynamic drag force and the aerodynamics lift force, where aerodynamic drag force and rolling resistance is pure *losses*, meanwhile the forces due to climbing resistance and acceleration are conservative forces with possibility to, partly, recover. This resultant force is the sum of all these acting forces, will produce a counteractive torque to the driving motor, Therefore disturbance torque to EV is the total resultant torque generated by the acting forces, by the computation of the resistant forces, it can be determined the needed torque at the wheel, and finally the rated torque of the electrical machine [34]. ***Gears modeling*** : *Gear* ensures the transmission of the motor torque to the driving wheels. The gear is modeled by the gear ratio *n* [35]

The total resultant force is the sum of all acting forces, and is given by:

$$F_{Total} = \mathrm{F}_{\mathrm{aerod}} + \mathrm{F}_{\mathrm{rolling}} + \mathrm{F}_{\mathrm{climb}} + \mathrm{F}_{angl\_acc} + \mathrm{F}_{lin\_acc} + \mathrm{F}_{w\ ind} \quad (3)$$

The wheels and axels convert F_{Total} and the speed of vehicle to torque, given by:

$$T_{Load} = r * F_{Total}$$

The needed energy of electric vehicle, the power that electric vehicle must develop at stabilized speed can be determined as the product of F_{total} multiplied by the speed of vehicle and given by:

$$P_{Total} = F_{Total} * \upsilon_{EV}$$

The power available in the wheels of the vehicle is expressed by:

$$P_w = T_e \frac{n * \upsilon_{EV}}{r}$$

The relationship between the tractive force and the torque produced by the motor

$$T_{load} = F_{Total} \frac{r}{n}$$

The driving force comes from the powertrain shaft torque, which can be written as the wheel torque, given by:

$$T_{wheel} = n * \eta * T_{shaft}$$

This wheel torque provides the resultant driving, tractive force, F_{Total} to the vehicle:

$$F_{Total} = \frac{T_{wheel}}{r} = \frac{n*\eta*T_{shaft}}{r}$$

The relationship between the resultant tractive force and the torque produced by the motor T_{shaft}, can be obtained as:

$$T_L = T_{shaft} = F_{Total} * \frac{r}{n*\eta}$$

To determine the electric battery capacity, and correspondingly design of the Photovoltaic panel with series and parallel connected cells, it is required to estimated energy required by EV, the required power in *kW* that must be develop at stabilized speed can be determined by multiplying the total force with the velocity of the EV, and given by :

$$P_{Total} = (\sum F)*\upsilon = F_{Total} * \upsilon$$

Electrical power (in watts) in a DC circuit can be calculated by multiplying current in Amps and *V* is voltage, and given by :

P= I x V

Based on fundamental principle of dynamics, the acceleration of vehicle is given by:

$$a = \frac{P_w - P_a}{M\upsilon} = \frac{T_e n - r*F_{Total}}{M\upsilon}$$

The angular velocity (Rad/sec), at the wheels, is given by

$$\omega_{wheel} = \frac{\upsilon_{EV}}{r}$$

The angular speed of electric motor (Rad/sec), is given by:

$$\omega_{motor\_shaft} = \frac{n}{r}\frac{da}{dt}$$

The relationship between the velocity of the vehicle, *v*, and the angular velocity of the electric motor is given by

$$\upsilon = \frac{r*\omega_{motor}}{n}$$

Modeling the acting on running vehicle forces: reference to [1, 24:26,34,],The acting on running vehicle forces are categorized into road-load and tractive forces and given as follows

Rolling resistance force, $F_{Rolling}$ is given by:

$$\mathrm{F_{Rolling}} = F_{normal\_force} * \mathrm{C_r} = M*g*\mathrm{C_r}*\cos(\alpha) \qquad (4)$$

For motion on a level surface, $\alpha=0$, $\cos(\alpha)=1$, and Eq.(4) becomes:

$$\mathrm{F_{Rolling}} = M*g*\mathrm{C_r}$$

In terms of the vehicle linear speed Eq.(4) becomes:

$$\mathrm{F_{Rolling}} = \mathrm{M}*\mathrm{g}*(\mathrm{C_{r0}}\text{-}\mathrm{C_{r1}}*\upsilon)*sign(\upsilon)$$

Where : C_r, C_{r1} The rolling resistance coefficients. C_r are calculated by expression given by Eq.(5) (C_r = 0.01828).:

$$\mathrm{C_r} = 0.01\left(1+\frac{3.6}{100}\upsilon_{car}\right) \qquad (5)$$

The rolling resistance torque is given by:

$$\mathrm{T_{Rolling}} = (M*g*\mathrm{C_r}*\cos(\alpha))*r$$

Aerodynamic Drag force , F_{aerod}: takes into account the aerodynamics of the vehicle and is function of car linear velocity, *v* and given by:

$$\mathrm{F_{aerod}} = 0.5*\rho*\mathrm{A}*\mathrm{C_d}*\upsilon_{vehicl}^2 \qquad (6)$$

Considering car and wind speed Eq.(6) become:

$$\mathrm{F_{aerod}} = 0.5*\rho*\mathrm{A}*\mathrm{C_d}*(\upsilon_{vehicl}+\upsilon_{wind})^2 * sign(\upsilon_{vehicl}+\upsilon_{wind})$$

$$\mathrm{F_{aerod}} = 0.5*\rho*\mathrm{A}*\mathrm{C_d}*(\upsilon_{vehicl}+\upsilon_{wind})^2$$

The aerodynamics torque is given by:

$$\mathrm{T_{aerod}} = \left(\frac{1}{2}*\rho*\mathrm{A}*\mathrm{C_d}*\upsilon_{vehicl}^{\ 2}\right)*r$$

Where: C_d : Aerodynamic drag coefficient characterizing the shape of the vehicle, empirically determined, for each specific vehicle. Considering shape of EV platform as cylinder▭, the aerodynamic drag coefficient is found from aerodynamic force as follows,: the drag force is found by $F_a = \tau_m * A$, where : τ_m :shear stress and found by equation $\tau_m = \mu\,(\mathrm{du}/\mathrm{dy})|_{y=0}$. Where: μ: air dynamic viscosity $1.5x10^{-5}$. A: frontal area of EV platform (A=*1.2*1=1.2 m^2*). ν: EV linear speed of (23 *m/s*), substituting and calculating we find Aerodynamic drag coefficient C_d =0.80. C_d is not an absolute constant for a given body shape, it varies with the speed of airflow (or more generally with Reynolds number R_e. v_o : The speed of the wind (*m/s*), against the direction of the platform's motion, *r*: wheel radius *0.3 m*. ρ: The air density (*kg/m^3*) at STP, ρ =1.25, At 20°C and 101 *kPa*, ρ =1.2041. The air density is calculated by below expression, where: ρ_o = 101325 *Pa*, sea level standard atmospheric pressure, T_0 = 288.15 *K* sea level standard temperature. g = 9.81 m/s^2. Earth-surface gravitational acceleration. L = 0.0065 *K/m* temperature lapse rate. R = 8.31447 *J/(mol*K)* universal gas constant. M = 0.0289644 *kg/mol* molar mass of dry air.

$$\rho = \frac{M_o*\rho_0\left(1-\frac{L*h}{T_O}\right)^{\frac{g*m}{R*L}}}{R*T}$$

The aerodynamics lift force, F_{lift}; is caused by pressure difference between the vehicle's roof and underside, and is given by:

$$F_{lift} = 0.5*\rho*C_L*B*\upsilon^2$$

The coefficient of lift C_L, with values(C_L to be 0.10 or 0.16), can be calculated using expression given by:

$$C_L = \frac{L}{0.5\rho\upsilon^2 A}$$

The force of wind , F_{wind} ; can be calculated by:

$$\mathrm{F_{wind}} = 0.5*\rho*\mathrm{A}*\mathrm{C_d}*(\upsilon_{vehicl}+\upsilon_{wind})^2$$

Also, the resistant force due to wind, cannot be precisely computed. It depends on various conditions, like (for common automobiles) the fact that windows are entirely or partially open etc... Also, the wind will never blow at constant speed. However, an expression, determined empirically, which will take into account the speed of wind, ν_{wind}, can be written as

$$\mathrm{F_{wind}} = \mathrm{F_{aerod}}\left(\mathrm{K}_{wind}\left[0.98\left(\frac{\upsilon_{wind}}{\upsilon}\right)^2 + 0.63\left(\frac{\upsilon_{wind}}{\upsilon}\right)\right] - 0.4\left(\frac{\upsilon_{wind}}{\upsilon}\right)\right)$$

Where: K_{wind} is the wind relative coefficient, depending on the vehicle's aerodynamics, (here K_{wind} =1.6) [36].

The hill-climbing resistance force , F_{climb} ; based on angle of incline α, it is given by:

$$\mathrm{F_{climb}} = M*g*\sin(\alpha)$$

For small angles, $\sin(\alpha) \approx \tan(\alpha)$, and $\tan(\alpha) = g$, correspondingly

$$\mathrm{F_{climb}} = Mg$$

The hill-climbing resistance, *slope*, torque, is given by:

$$\mathrm{F_{climb}} = \mathrm{F_{slope}} = (M*g*\sin(\alpha))*r$$

The normal force F_{norm} is the force exerted by the road on the vehicle's tires, the magnitude of F_n equals the magnitude of the F_{acc} in the direction normal to the road, The normal force F_{norm} can be found as by:

$$\mathrm{F_{norm}} = F_{climb} - F_{lift} = (M*g*\sin(\alpha)) - (0.5*\rho*C_L*B*\upsilon^2)$$

The linear acceleration force F_{acc} , , is the force required to increase the speed of the vehicle, can be described as a linear motion given by:

$$\mathrm{F}_{\mathrm{acc}} = M * a_{EV} = M \frac{d\upsilon_{EV}}{dt} = \left(M + \frac{J_{wheel}}{r^2} \right) \frac{d\upsilon_{EV}}{dt}$$

$$\mathrm{F}_{\mathrm{acc}} = M * a = M \frac{d\omega}{dt} = M \frac{\sum T}{J}$$

The angular acceleration force F_{acc_angle} , is the force required by the wheels to increase the speed of the vehicle to make angular acceleration and is given by:

$$\mathrm{F}_{\mathrm{acc\_angle}} = J \frac{n^2}{r^2} a$$

The angular acceleration torque is given by:

$$T_{\mathrm{acc\_angle}} = r * J \frac{n^2}{r^2} a = J \frac{n^2}{r} a$$

Based on these derived forces and corresponding torques, the following expressions can be proposed for total force, such that can be used to develop Simulink sub-model.

$$F_{Total} = M\upsilon + M\upsilon g \sin(\alpha) + sign(\upsilon) Mg \cos(\alpha) C_r + sign(\upsilon + \upsilon_{wind}) 0.5 \rho C_d A (\upsilon + \upsilon_{wind})^2$$

Or

$$F_{Total} = 0.5 * \rho * \mathrm{A} * \mathrm{C_d} * \upsilon_{vehicl}^2 + M * g * \mathrm{C_r} * \cos(\alpha) + M * g * \sin(\alpha) + J \frac{n^2}{r^2} a + \left(M + \frac{J_{wheel}}{r^2} \right) \frac{d\upsilon}{dt} +$$

$$+0.5 * \rho * C_L * B * \upsilon^2 + \mathrm{F_{aerod}} \left(\mathrm{K}_{wind} \left[0.98 \left(\frac{\omega_{wind}}{\upsilon} \right)^2 + 0.63 \left(\frac{\omega_{wind}}{\upsilon} \right) \right] - 0.4 \left(\frac{\omega_{wind}}{\upsilon} \right) \right)$$

2.4.1 Energy source modeling

The batteries are devices with high specific energy. The main purpose of the battery is to provide all the power needed for acceleration and accessories such as clocks, security systems, automatic diagnostic systems, vent fans, ignition systems, entertainment systems, air conditioning, heating, etc. Traction batteries for electric vehicles are usually specified as 6V or 12 V, and these units are in turn connected in series to produce the voltage required. This voltage will, in practice, change. When a current is given out, the voltage will fall; when the battery is being charged, the voltage will rise. Two battery types are preferred EV; Nickel Metal Hydride (NiMH) and Lithium Ion. The battery is modeled as a voltage source with an internal resistance. The Lithium-Ion type battery current is calculated as given by Eq.(7)[35]. The equivalent circuit of a battery is shown in Figure 8. The battery is represented as having a fixed voltage *E*, but the voltage at the terminals is a different voltage *V* , because of the voltage across the internal resistance *R*. Assuming that a current *I* is flowing out of the battery, then by basic circuit theory we can say tha:

$$I_{Battery} = \frac{V_{oc} - \sqrt{V_{oc}^2 - 4(\mathrm{R}_{in} + \mathrm{R}_t)\mathrm{P}_b}}{2(\mathrm{R}_{in} + \mathrm{R}_t)} \qquad (7)$$

Where: P_b: battery output power, R_{int} : Internal resistance , V_{oc}: the open circuit voltage , R_t

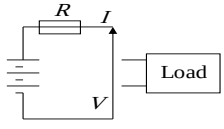

Figure 8 Battery Simplified equivalent circuits, consisting of thee units connected in series to result in 36 V

2.5 Selecting and Modeling of electric Machine

The selection of driving Machine (motor) for a specific EV is dependent on many factors, such as the intention of the EV, correspondingly allowable variation in speed and torque and ease of control. HSEV requires that the driving electric machine has a wide range of speed regulation. In order to guarantee the speed-up time, the electric machine is required to have large torque output under low speed and high over-load capability, and in order to operate at high speed, the driving motor is required to have certain power output at high-speed operation [37-38]. For propulsion usually the induction machine (IM), permanent magnet synchronous machine (PMSM), and switched reluctance machine (SRM) are considered [38]. Systems based on PM machines represent a competitive solution for actual performance of automotive and naval applications . Compared to other electrical machines, PM machines combine the advantages (attracting the interest of EV industry) of high efficiency, power factor and torque density, high overload capability, robustness, reduced maintenance, compactness and low weight , high reliability and maintenance-free. High energy PM exciting allows reducing overall volume (i.e. weight) and stator losses. On the other hand, the absence of rotor copper losses allows a further increase of the efficiency. Also fault-tolerant capability , flux-weakening capability [39-40], and low short-circuit current could be obtained . The "best" choice among proposed machines, beside above mentioned, is like many other components is a trade off between, cost, mass, volume, efficiency, reliability, maintenance, [41] and ease of control etc. However, due to its high power density and high efficiency the PMSM have found and is selected for wide applications in various fields. In [42-43] Most used in Mechatronics Applications DC machine are mathematical described and corresponding Simulink models are developed and tested.

The dynamic equations of motors can be derived, mainly based on the Newton's law combined with the Kirchoff's law. The fundamental system of electromagnetic equations for any electric motor is given by [1,16-17]

$$\left.\begin{aligned} u_s &= R_s i_s + \frac{d\psi_s}{dt} + j\omega^k \psi_s \\ u_s &= R_R i_R + \frac{d\psi_R}{dt} + j(\omega^k - P_b \omega_m)\psi_R \\ \psi_s &= L_s i_s + L_\mu i_R \\ \psi_R &= L_R i_R + L_\mu i_S \end{aligned}\right\} \qquad (8)$$

Where : ω^k the angular speed of rotating coordinate system (reference frame), Depending on motor construction (AC or DC), the method of the supply and the coordinate system (stationary or rotating with the rotor or stator flux) the above mentioned model becomes transformed to the desirable

form[1][44], and the complement Eqs. (1) is equations describing mechanical part of eclectic motor.
The d-q model of PMSM Voltage equations are given by:

$$V_d = R_s * i_d + L_d \frac{di_d}{dt} - \omega_e L_q * i_q$$

$$V_q = R_s * i_q + L_q \frac{di_d}{dt} + \omega_e L_d * i_d + K_b \omega_m$$

Electric input power

$$P = \frac{3}{2}\left(V_d i_d + V_q i_q\right)$$

The mechanical part of the PMSM can be modeled as follows:
The electromechanical torque is given by:

$$T_e = J_{shaft} \frac{d\,\omega_{shaft}}{dt} + B\,\omega_{shaft} + T_{coulomb} + T_{shaft}$$

$$P = T_{shaft}\,\omega_{shaft}$$

The coupling between the electric and mechanic part is given by:

$$T_e = \frac{3}{4} P(\lambda_{PM}\, i_q + (L_d + L_q) i_q i_d)$$

The equations giving the stator current can be written in the following form:

$$I_d = \frac{1}{L_d s + r}\left(V_d + \omega_e L_q * i_q\right)$$

$$I_q = \frac{1}{L_q s + R}\left(V_q + \omega_e L_d * i_d - K_b \omega_m\right)$$

The electromagnetic torque developed by the motor is given by:

$$T_m = \frac{3K_b I_q}{2} + 0.5 * P(L_d I_d I_q - L_q I_d I_d)$$

Where P: number of poles, λ_{pm}: Permanent magnet flux linkage (W),L_q: Q-axis inductance(H), L_d :D-axis inductance(H), V_d: D-axis voltage(V), V_q: Q-axis voltage (V), i_d: D-axis current(A), i_q: Q-axis current (A),
Different resources introduce equivalent block diagram model for PMSM motor including [44]. Equivalent block diagram of PMSM motor, shown in figure 9(a) can used in the proposed EV system model, it is equivalent PMDC motor, is shown in figure 9(b) can be used for the proposed EV system's model, A detailed mathematical description and Simulink models of DC machine has been studied for last decades, and can be found in different resources including [1][12-19][28]. Correspondingly, the DC motor system dynamics will have the form given by Eq.(9). The coulomb friction can be found at steady state, *to be* as by Eq.(10)*:*

$$K_t\, i_a = T_\alpha + T_\omega + T_{load} + T_f \quad (9)$$

$$K_t\, i_a - b*\omega = T_f \quad (10)$$

Since geometry of the mechanical part determines the moment of inertia, and EV system is considered to be of is cylindrical shape with the inertia calculated as given by Eq.(11) , where the total equivalent inertia, J_{equiv} and total equivalent damping, b_{equiv} at the armature of the motor with gears attaches, are given by Eq.(11). It is supposed, that the total equivalent inertia, J_{equiv} contains the inertias of the vehicle, of the DC machine, the gears and the driven wheels.

$$b_{equiv} = b_m + b_{Load}\left(\frac{N_1}{N_2}\right)^2 \quad \Leftrightarrow \quad J_{equiv} = J_m + J_{Load}\left(\frac{N_1}{N_2}\right)^2 \quad (11)$$

$$J_{load} = \frac{bh^3}{12} \Leftrightarrow J_{equiv} = J_{motor} + J_{gear} + J_{veh} + (J_{wheel} + mr^2)\left(\frac{N_1}{N_2}\right)^2$$

From the energy conservation principle, the following are derived [45]:

$$0.5M\,\upsilon^2 = 0.5J_{veh}\omega^2 \Rightarrow 0.5J_{veh}\omega^2 = \frac{M\,\upsilon^2}{\omega^2}$$

where: $\omega = n\omega_{wheel}$, $\upsilon = r\omega_{wheel} = \frac{r\omega}{n}$

Substituting and manipulating, gives:

$$J_{veh} = \frac{M \cdot r^2 \cdot \omega^2}{n^2 \cdot \omega^2} = M\,\frac{r^2}{n^2}$$

The disturbance torque, *T*, is all torques including coulomb friction, and given by Eq.(12). w*here:* T_{Load} is the torque of all acting forces .Correspondingly, the equivalent EV's open-loop transfer function is given by Eq.(13):

$$T = T_{Load} + T_f \quad (12)$$

$$G_{open}(s) = \frac{\omega_{platform}(s)}{V_{in}(s)} = \quad (13)$$

$$= \frac{K_t / n}{\left(L_a s + R_a\right)\left(J_{equiv} s^2 + b_{equiv} s\right) + \left(L_a s + R_a\right)\left(T\right) + K_b K_t}$$

Considering that the DC motor subsystem dynamics and disturbance torques depends on mobile platform shape and dimensions, in modeling DC motors and in order to obtain a linear model, the hysteresis and the voltage drop across the motor brushes is neglected, other DC motors types can be used, where the input voltage, V_{in} maybe applied to the field or armature terminals [28].

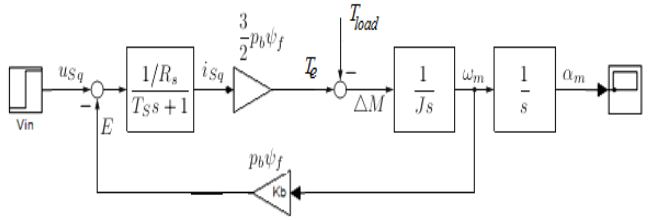

Figure 9 (a) Equivalent block diagram (Simulink model) of PMSM)[1]

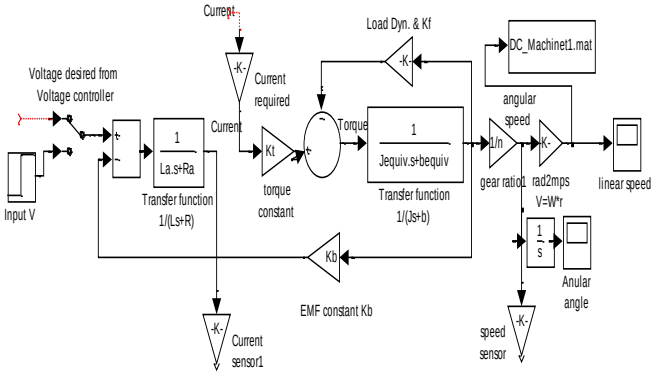

Figure 9 (b) Simulink model of the open loop EV PMDC machine system and proposed current and speed control components [1]

2.5 Selection and Modeling of sensing device

When the pedal is pushed, the controller delivers electrical currents from the battery to the motor; this gives the car acceleration to accelerate to the desired output speed, the sensors sense the actual output speed and fed it back to controller. Tachometer is a sensor used to measure the actual output angular speed, ω_L. Dynamics of tachometer can be represented using Eq.(14), assuming the SEV system, is to move with maximum linear velocity of 23 m/s, (that is 82.8 km/h), EV's wheel radius of 0.25 m the angular speed is

obtained as shown by Eq.(15). Therefore, the tachometer constant, for calculated angular speed ω, is given as shown by Eq.(15).

$$V_{out}(t) = K_{tach}\frac{d\theta(t)}{dt} \Rightarrow \quad (14)$$

$$V_{out}(t) = K_{tach}\omega \Rightarrow K_{tach} = \frac{V_{out}(s)}{\omega(s)}$$

$$\omega = \frac{v}{r} = \frac{23}{0.25} = 92 \text{ rad/s} \quad \Rightarrow \quad (15)$$

$$K_{tach} = \frac{12}{92} = 0.13043 = 0.13$$

2.5.1 Modeling the relation between throttle and speed

Throttle ,known as the "accelerator" or "gas pedal" , controls voltage supply to the vehicle's DC Machine and correspondingly controls the DC Machine output, were pressing the accelerator increases the angular speed of DC machine . In standard operation the gas pedal angle is controlled by the driver, this relation can be represented mathematically as given by Eq.(16) were the maximum output linear speed is assumed to be 82.8 km/h, and the pedal angle is assumed to be between 0 and 45, the input will be the throttle angle . also, the driver can control the torque by means of a single accelerator pedal, where at zero per cent pedal (off throttle), the torque demand must be less than or equal to zero; at one hundred per cent pedal (full throttle), the torque demand must match or exceed the maximum torque output of the DC Machine in its current state .

$$K_{pedal} = \frac{Dv}{D\theta} = \frac{23}{45} = 0.5111 \quad (16)$$

2.6 Selection , Modeling and design of SEV control systems

Controlling the performance of SEV is not a simple task, where the design and operation parameters of SEV, as well as the road condition are always varying. SEV must to be designed and controlled to maximize the net power from solar panels, consume minimum electric power, while maintaining main characteristics of efficiency in driving the distance using the least amount of energy, quick, quiet motion and acceleration (smooth driving for comfortable riding), the best control strategy for this purpose, is to include separate and different vehicle and PVPC subsystems currents, voltage and motion controllers. For controlling the performance of SEV, the controller should be designed to make the system robust, adaptive and improving the system on both dynamic and steady state performances (fast responsive and low-ripple). **PI controller:** because of its simplicity and ease of design, PI controller is widely used in variable *speed* applications and *current* regulation, in this paper different and separate PI controller configurations will be applied for achieving desired outputs characteristics of PVPC subsystem and meeting desired output speed of whole EV system,. The *PI* controller transfer function in different forms is given by Eq.(17). The PI controller pole/zero configurations will affect the response, mainly the PI zero given by; $Z_o=-K_I/K_P$, will inversely affect the response and should be cancelled by prefilter, while maintaining the proportional gain (K_P), the prefilter transfer function is given by Eq.(18) , the placement of prefilter is shown on generalized system model.

$$G_{PI}(s) = K_P + \frac{K_I}{s} = \frac{(K_P s + K_I)}{s} = \frac{K_P\left(s + \frac{K_I}{K_P}\right)}{s} = \frac{K_P(s + Z_o)}{s} = \quad (17)$$

$$G_{PI}(s) = K_{PI} * \frac{(T_I s + 1)}{T_I s} = K_{PI} * \left(1 + \frac{1}{T_I s}\right)$$

$$G_{Prefilter}(s) = \frac{Z_O}{(s + Z_O)} = \frac{Z_{PI}}{(s + Z_{PI})} \quad (18)$$

2.6.1 Control algorithm selection, Modeling and design for electric machine subsystem

There are many motor control system strategies that may be more or less appropriate to a specific type of application each has its advantages and disadvantages; the designer must select the best one for specific application. Different control algorithms are introduced in different resources for controlling EV including [1][34][45]. The proposed EV control system composed of two loops, inner and outer; The first loop is ***inner current regulation loop*** that accomplishes current regulation control to meet the current needs in accordance with the needs of electric vehicle, and the second loop is ***outer speed regulation loop*** that adjusts the speed of the motor (see Figure 9). Different control algorithms can be applied including fuzzy, PID, PI, PI with deadbeat design.

The SEV speed controller: Speed controller takes the nominally fixed voltage from the power source (battery) and outputs a variable voltage supply needed to control the motor speed. Its voltage output to the drive motors changes in response to control signals supplied by the user from foot pedal [8].When the pedal is pushed, the controller delivers electrical currents from the battery to the motor; this gives the car acceleration to accelerate to the desired output speed, the sensors sense the actual output speed and fed it back to controller. the main voltage conversion is done very efficiently using PWM technique, where controller sends pulses of power to the motor thousands of times per second, where very short pulses cause the motor to go slowly and long pulses cause the motor to go fast. In [1] PID, PI controller and PI-controller with deadbeat response design are applied in controlling the output speed of EV, a suitable selection is PI controller .

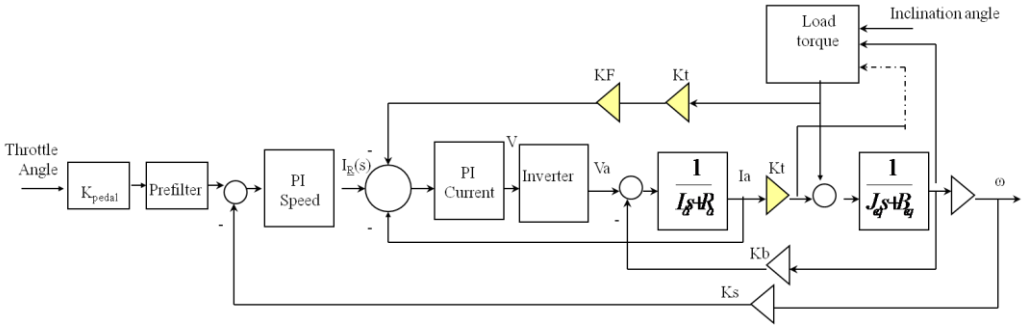

Figure 9 Proposed control scenario

www.ijecs.in
International Journal Of Engineering And Computer Science ISSN:2319-7242
Volume 3 Issue 9, September 2014 Page No. 8418-8438

The outer Speed regulator controller: shown in Figure 9 and Figure 10(a). In order to have smooth driving for comfortable riding, no steady state error and acceptable anti-disturbance capability at transient state, a suitable selection is PI controller with transfer function given by:

$$G_{PI\_speed}(s) = \frac{\left(K_{P\_\omega}s + K_I\right)}{s} = \frac{K_{P\_\omega}\left(s + \frac{K_{I\_\omega}}{K_{P\_\omega}}\right)}{s}$$

$$G_{PI\_speed}(s) = K_{P\_\omega} * \frac{(T_\omega s + 1)}{T_\omega s} = K_{P\_\omega} * \left(1 + \frac{1}{T_\omega s}\right)$$

Where, K_{P_ω}: the proportional coefficient of speed regulator; K_{I_ω}: the integral coefficient of speed regulator; T_ω: time constant of motor speed. Depending upon generic open loop transfer function, the parameters of speed controller loop can be found to be:

$$K_{P\_\omega} = \frac{J}{2T_c} \Rightarrow K_{I\_\omega} = \frac{K_P}{4T_c}$$

Where: T_c is the sum time delay due to speed loop, The same approach, with PI prefilter to cancel the zero, can be applied to speed loop PI controller.

The SEV current controller should be designed to maintain the main characteristics of efficiency in driving the distance using the least amount of energy, and supply the motor with corresponding current corresponding to load variations and desired acceleration. *Current inner controller loop:* guarantees limited variations of the current trough the inductor during important load variations. The current regulation loop is the inner loop connected to the stator circuit; this is shown in DC machine subsystem sub-model shown in Figure 10(c). In this paper we are to design current regulator as PID or PI controller. In order to have minimum overshoot and good tracking performance current regulation can be designed as type-I system. In case current controller is designed as PI regulator, the parameters of PI current controller can be designed as the follows:

The motor voltage can be written as:

$$(L_a s + R_a)\, I(s) = V_{in}(s) - K_b\, s\theta(s)$$

The Laplace transformed equation of motor stator circuit, in terms of input voltage $V_{in}(s)$ and output current, $I(s)$ is given by:

$$\frac{I(s)}{V_{in}(s) - K_b s\theta(s)} = \frac{1}{(L_a s + R_a)} \qquad (19)$$

In practical systems, due to the fact that the electromagnetic time constant is smaller than electromechanical time constant, current regulation is faster than speed regulation. Hence, speed regulation is faster than the variation of back EMF, therefore, the effect of back EMF on current regulation loop can be neglected, therefore Eq. (19), can be rewritten as

$$\frac{I(s)}{V_{in}(s)} = \frac{1}{(L_a s + R_a)}$$

In terms of time constant, motor stator circuit will have the form:

$$\frac{I(s)}{V_{in}(s)} = \frac{1/R_a}{(T_{electric} s + 1)}$$

Where : $T_{electric}$ electrical motor (stator circuit) time constant. Depending on [46-47] , the open loop transfer function of current loop is given by:

$$G_{current\_loop}(s) = \frac{K_P}{(R_a T_{electric})s} \frac{1}{(2T_s s + 1)}$$

The parameters of PI current controller can be deduced depending upon generic open loop transfer function with damping factor ζ=0.707and given by:

$$G_{generic}(s) = \frac{1}{2\xi s(\xi s + 1)}$$

$$K_P = \frac{R_a T_{electric}}{4T_s} \Rightarrow K_I = \frac{K_P}{T_{electric}}$$

Therefore, the current regulator transfer function, PI controller, is given by:

$$\frac{\left(K_{P\_current}s + K_I\right)}{s} = \frac{K_P\left(s + \frac{K_{I\_current}}{K_{P\_current}}\right)}{s} =$$

$$G_{PI\_current}(s) = K_{P\_current} * \frac{(T_I s + 1)}{T_I s} = K_{P\_current} * \left(1 + \frac{1}{T_I s}\right)$$

Where: $K_{P\_current}$: the proportional gain; $K_{I\_current}$: integral gain; T_I: time constant of current regulator. Mainly the PI zero, Z_o=-K_I/ K_P, will inversely affect the response and it could be cancelled by prefilter, the required prefilter transfer function to cancel the zero is given by:

$$G_{Prefilter}(s) = \frac{Z_o}{(s + Z_o)} = \frac{1/T_I}{(s + 1/T_I)}$$

The inverter: The input voltage V_{in} to inverter is considered as constant (36 V), the main voltage conversion is done very efficiently using PWM techniques, the output voltage is adjustable via the duty cycle α ,of the PWM signal. The transfer function of the inverter can be given as in [6] The PI current controller is affecting the inverter switching frequency to reduce the ripples in the torque and current

$$G_{converter}(s) = \frac{K_{PWM}}{T_s s + 1}$$

Where: K_{pwm}: gain of inverter; T_s: time constant of PWM controller, (to be 0.25 ms)

2.6.1 Control algorithm selection, Modeling and design for PVPC subsystem

The power delivered by a PV system is dependent on the irradiance β, temperature T, and the current drawn from the cells V. To maximize a PV system's output power, it is

necessary continuously tracking the maximum power point (MPP) in the I-V characteristic of the PV system, a switch-mode power converter, can be used to maintain the PV's operating point at the Maximum Power Point MPP, The Maximum Power Point tracker MPPT, does this by controlling the PV array's voltage or current independently of those of the load.

Perturb and observe algorithm; A detailed Simulink model of perturb and observe algorithm is shown in Figure 10(c)**.**The V_{PV} and I_{PV} are taken as the inputs to MPPT unit, duty cycle D is obtained as output. In this perturb and observe algorithm a slight perturbation is introduced to the system. Due to this perturbation the power of the module changes. If the power increases due to the perturbation then the perturbation is continued in that direction, after the peak power is reached the power at the next instant decreases and hence after that the perturbation reverses. When the steady state is reached the algorithm oscillates around the peak point [49]

Also, A PI controllers, also can be used to control PV panel characteristics, where two separate PI controllers are used, first PI current controller shown in Figure 9, is used to match motor-current with required Load-torque (Variations) current to overcome, where both currents are compared and the difference is fed to PI controller to generate converter's output current in accordance with Duty cycle to match and generate required load current. A second PI voltage controller shown in Figure 9 used to control the converter's output voltage to match desired output voltage, by comparing desired converter output voltage (36 V) and actual converter's voltage, the difference is fed to PI controller to control the buck converter MOSFET switch according calculated duty cycle to result in desired voltage[45][48].

3. Simulation, testing and evaluation

Integrating all the sub-models of SEV system, will result in the whole SEV system model shown in Figure 10(a), this system whole system consists of two major subsystems; PV subsystem with sub-model shown in Figure 10(b), DC machine with dynamics and controllers subsystem with mask sub-model shown in Figure 10(c). The DC machine sub-model is developed as mask sub-model with integrated DC machine sub-model and dynamics sub-model of all acting forces and torques and shown in Figure 10(d). The PV sub-model is developed by integrating PV panel sub-model shown in Figure10 (e) and converter sub-model with PWM generator both shown in Figure 10(f), the integrated mask model is shown in Figure 10(g)(h). The proposed whole SEV system model and each sub-model are developed to allow designer to have the maximum output numerical visual and graphical data to select, model, simulate, analyze and evaluation the whole SEV system and each subsystem outputs characteristics and performance, for desired overall and/or either subsystem's specific outputs, under various PV subsystem input operating conditions, to meet particular SEV system requirements and performance. The obtained results show the simplicity, accuracy and applicability of the presented models to help in Mechatronics design of SEV system.

3.1. Testing, analysis and evaluation of whole SEV system.

With reference to testing a maximum speed of 23 m/s, (that is 82.8 km/h) in maximum of 10 seconds, and for all subsystems parameters defined in Table 2. Running Simulink model will result in response curves shown in Figure 11 where in Figure 11(a) are shown linear speed, acceleration, current and motor torque response curves of SEV. Meanwhile in Figure 11(b) are shown generated PV panel's output voltage and Converter's output voltage, the simulation numerical results of each sub-model for given operating conditions are listed in Table 1. these response curves and numerical visual data show that the PV panel generates 72 V that is fed to buck converter and using PWM generator are converter to 36 V, that is the converter generates the desired output voltage of 36 V to be fed to SEV system to achieve desired output linear speed of 23 m/s. PV panel V-I and P-V Characteristics for operating condition shown in Figure 11(c)(d),

Changing the disturbance torque, e.g. mass and/or inclination will result in, more current consumed to overcome the change in load torque, the SEV response curves of output speed, current, torque are shown in Figure 11(e), meanwhile, the converter output current to match load disturbance ,while maintaining the desired output performance, this is shown in Figure 11(f)

Conclusions

A refined model for Mechatronics design of SEV system is proposed and tested. The proposed model is developed for research purposes, application in educational process, and to help in facing the main top challenges in developing Mechatronics SEV systems; early identifying system level problems and ensuring that all design requirements are met, the whole system model and each sub-model are developed to allow designer to have the maximum output data to select, model, simulate, analyze and evaluation the overall SEV system and each subsystem outputs characteristics and performance, for desired overall and/or either subsystem's specific outputs, under various PV subsystem input operating conditions, to meet particular SEV system requirements and performance. The whole SEV system model and each subsystems models, were developed, tested and evaluated in MATLAB/Simulink, the obtained results show the simplicity, accuracy and applicability of the presented models to help in Mechatronics design of SEV system .

International Journal Of Engineering And Computer Science ISSN:2319-7242
Volume 3 Issue 9, September 2014 Page No. 8418-8438

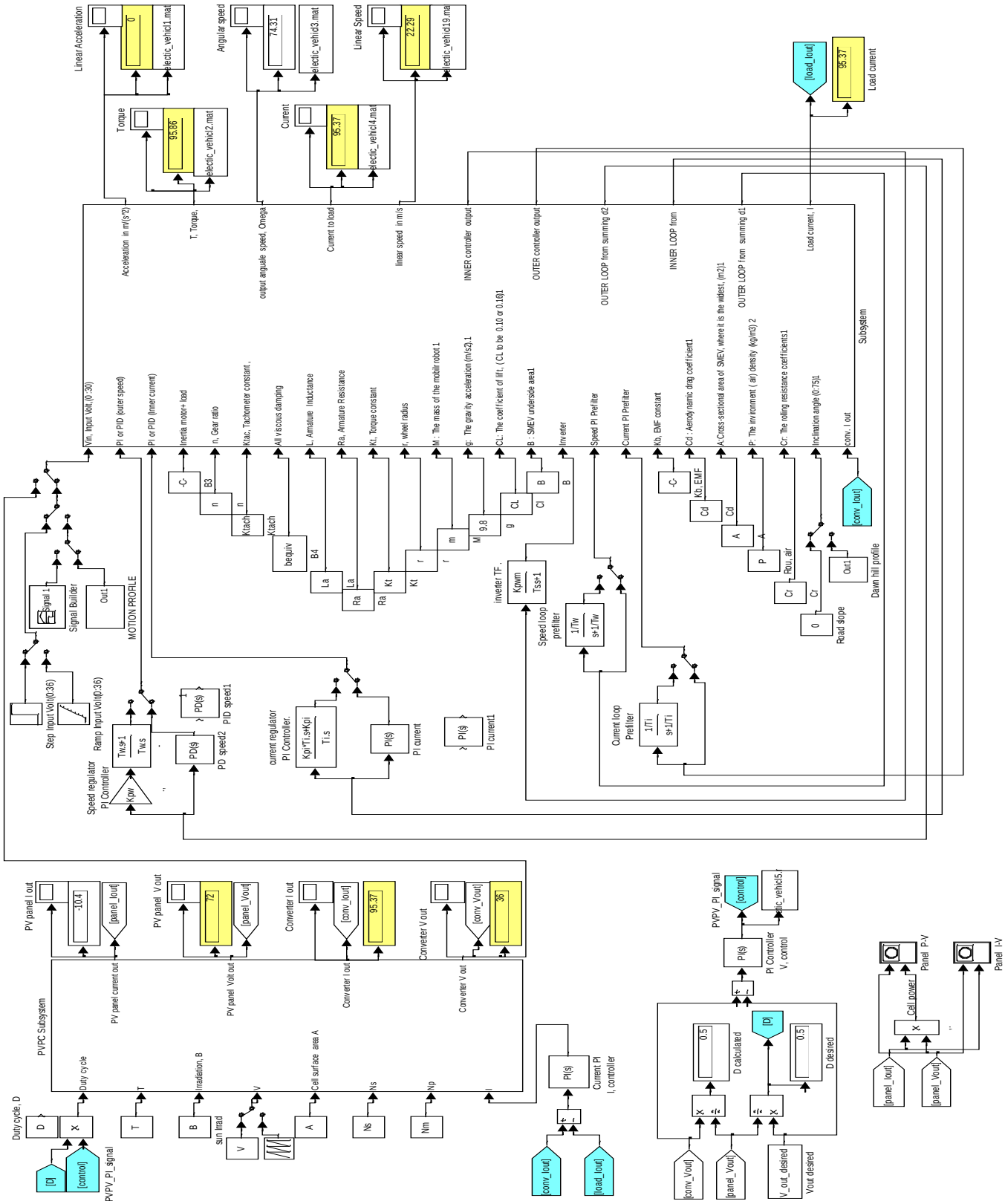

Figure 10(a) whole SEV system Simulink model

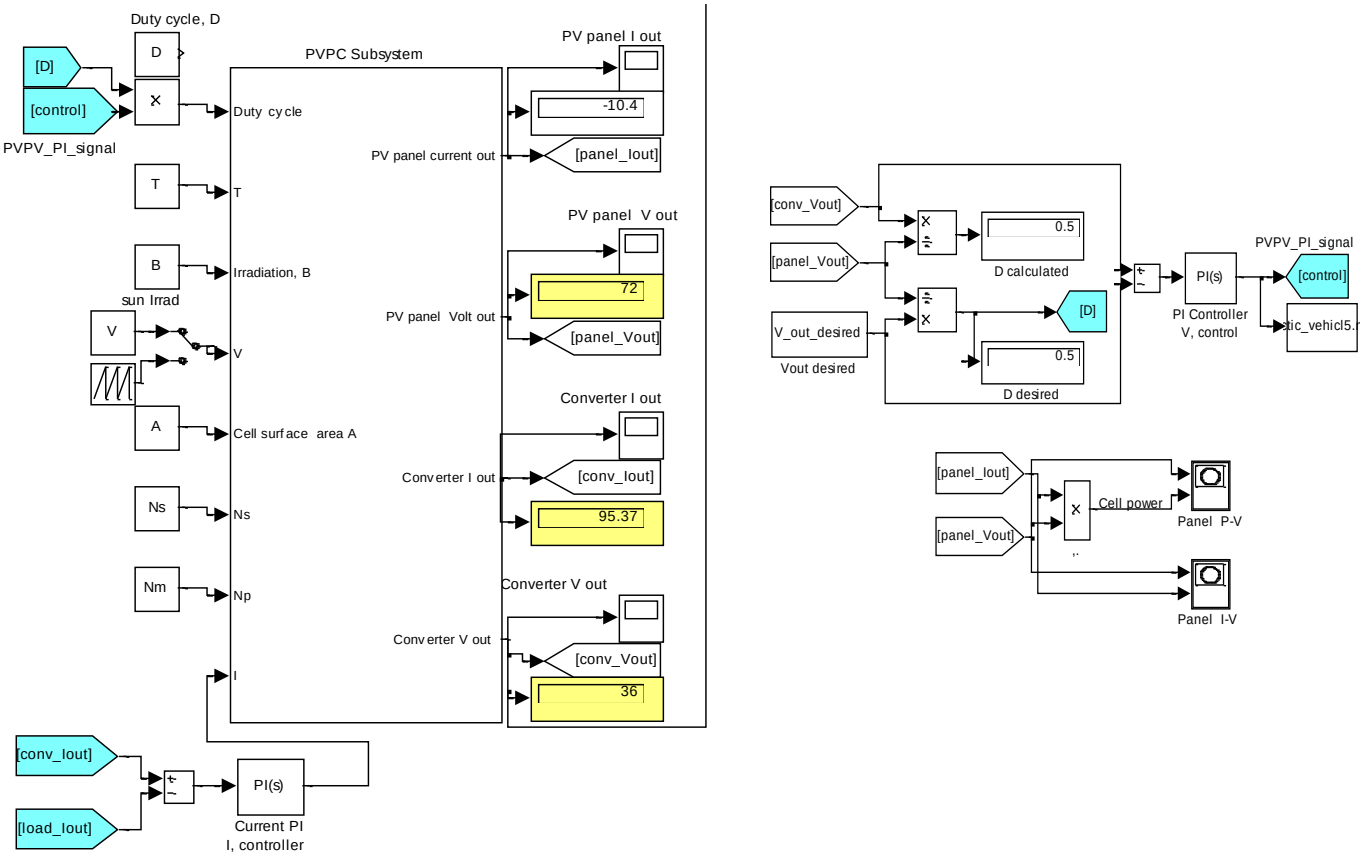

Figure 10(b) PV subsystem sub-model

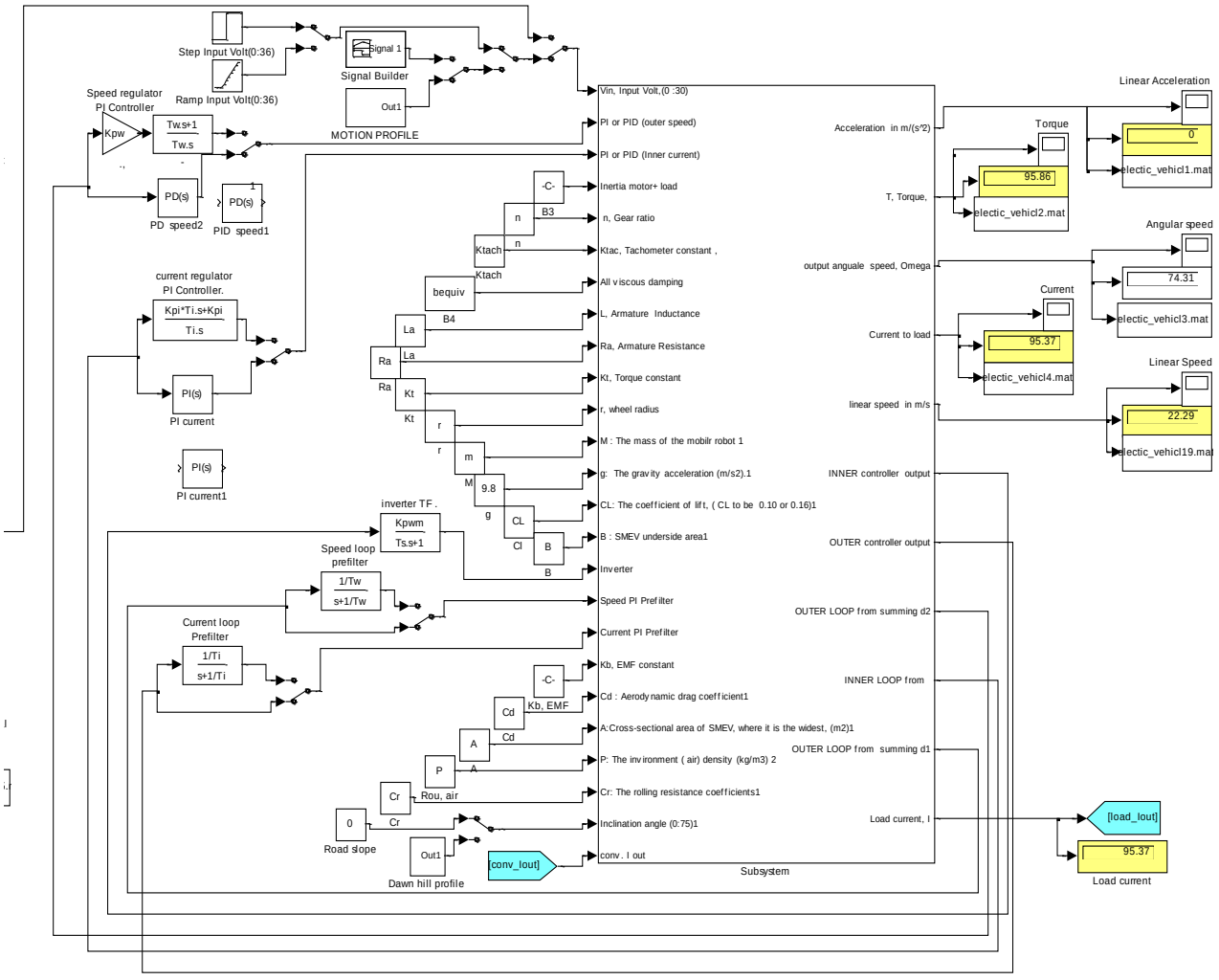

Figure 10(c) DC machine with dynamics and PI,PD controllers subsystems sub-models

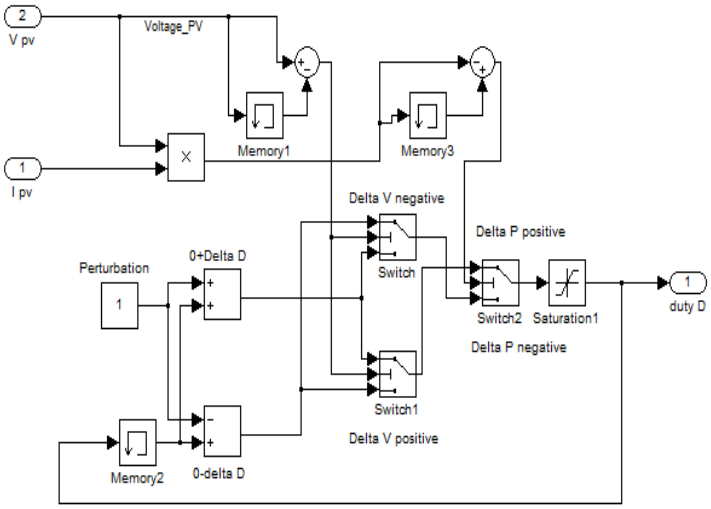

Figure 10(c) Perturb and Observe Algorithm simulation [49]

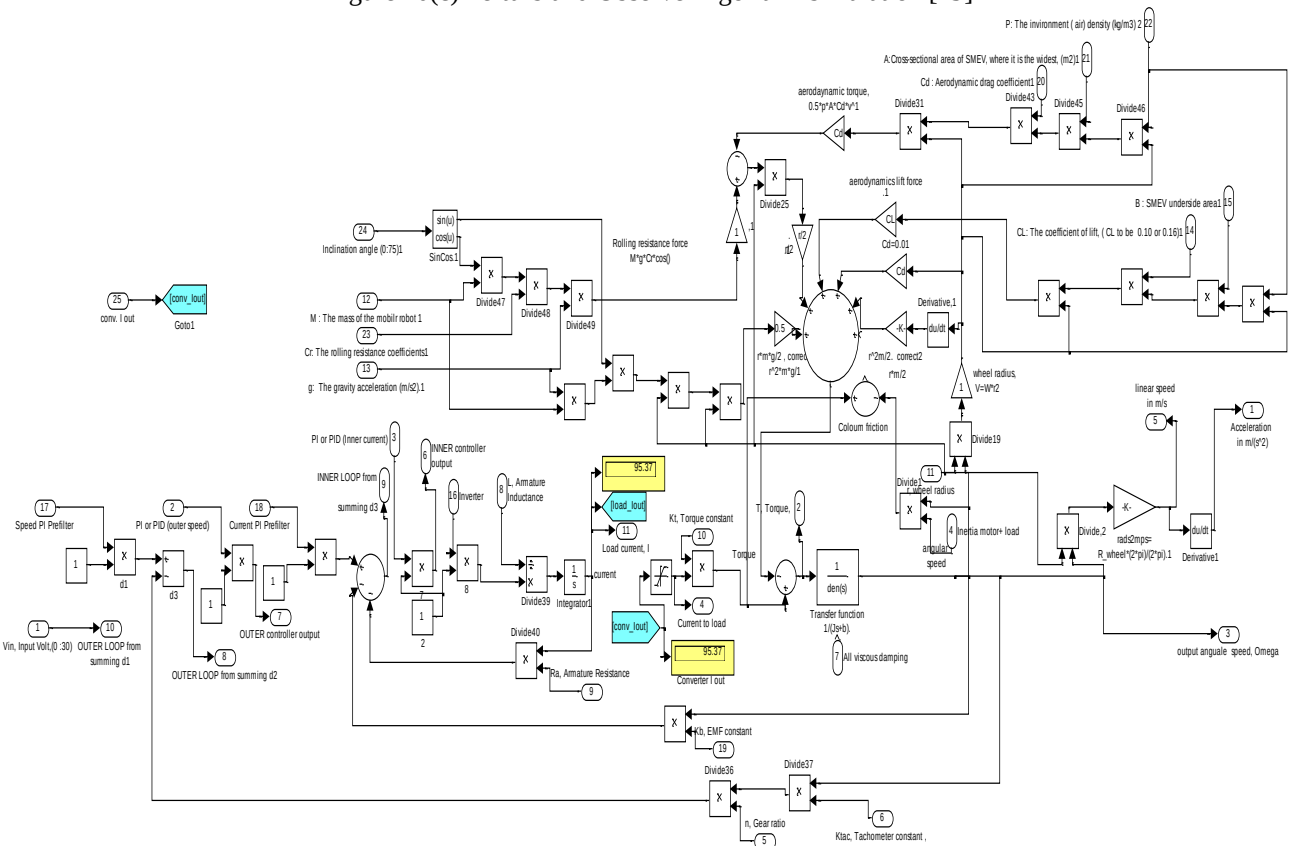

Figure 10(d) DC machine sub-model with dynamics and simulation of acting forces and torques and shown in

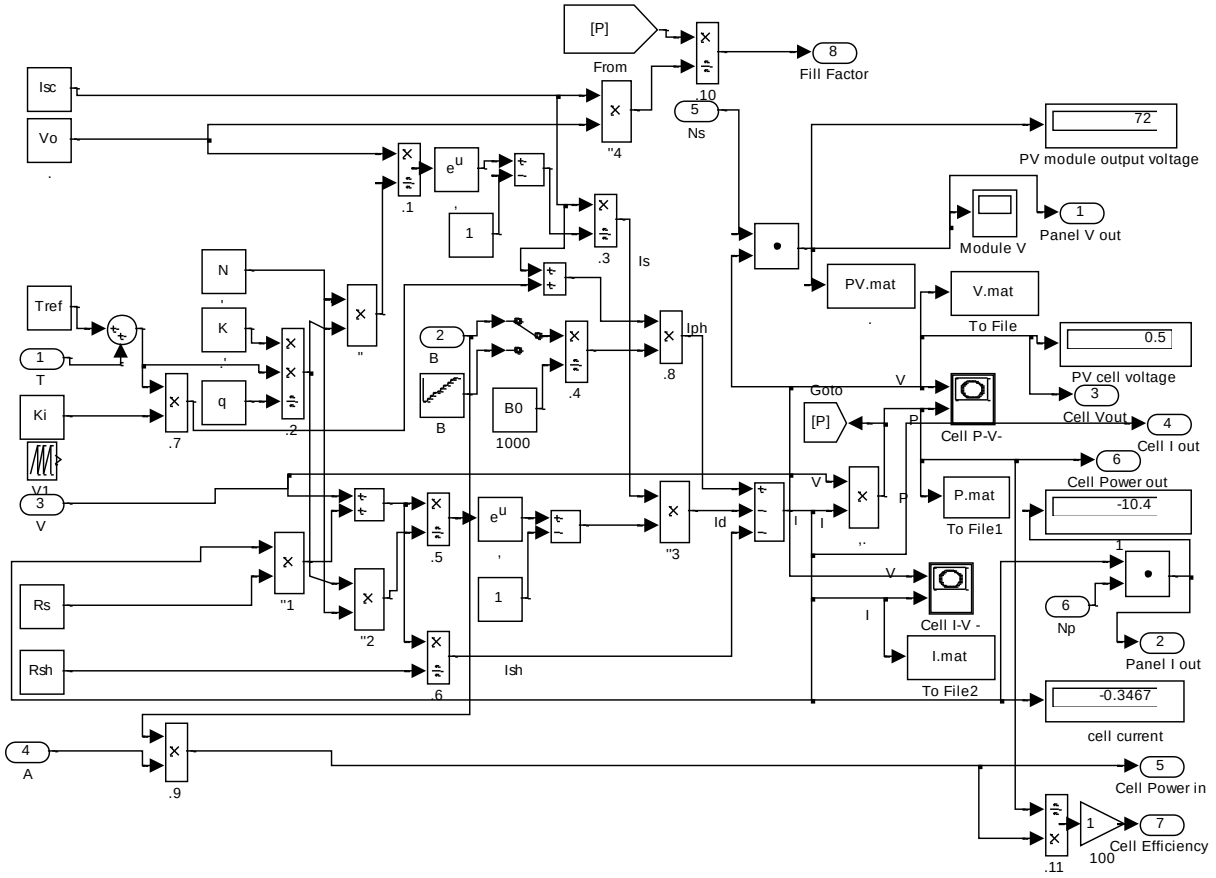

Figure 10(e) PV Panel sub-model

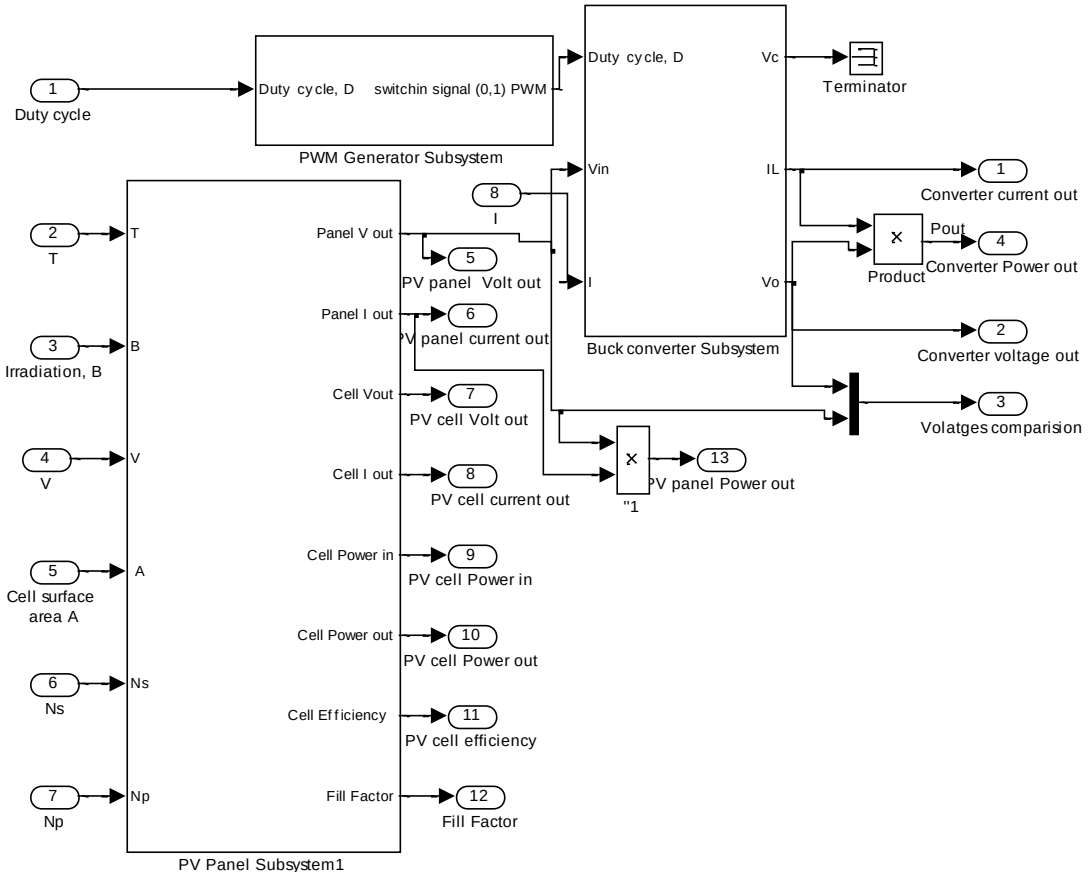

Figure 10(g) integrating PV panel sub-model and Converter sub-model in one sub-model

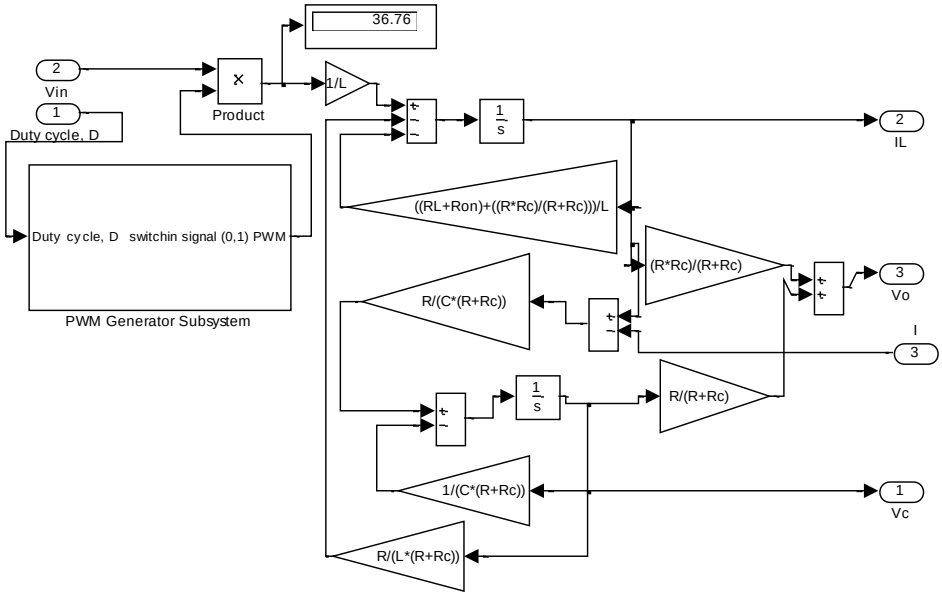

Figure 10(f) Buck converter sub-model

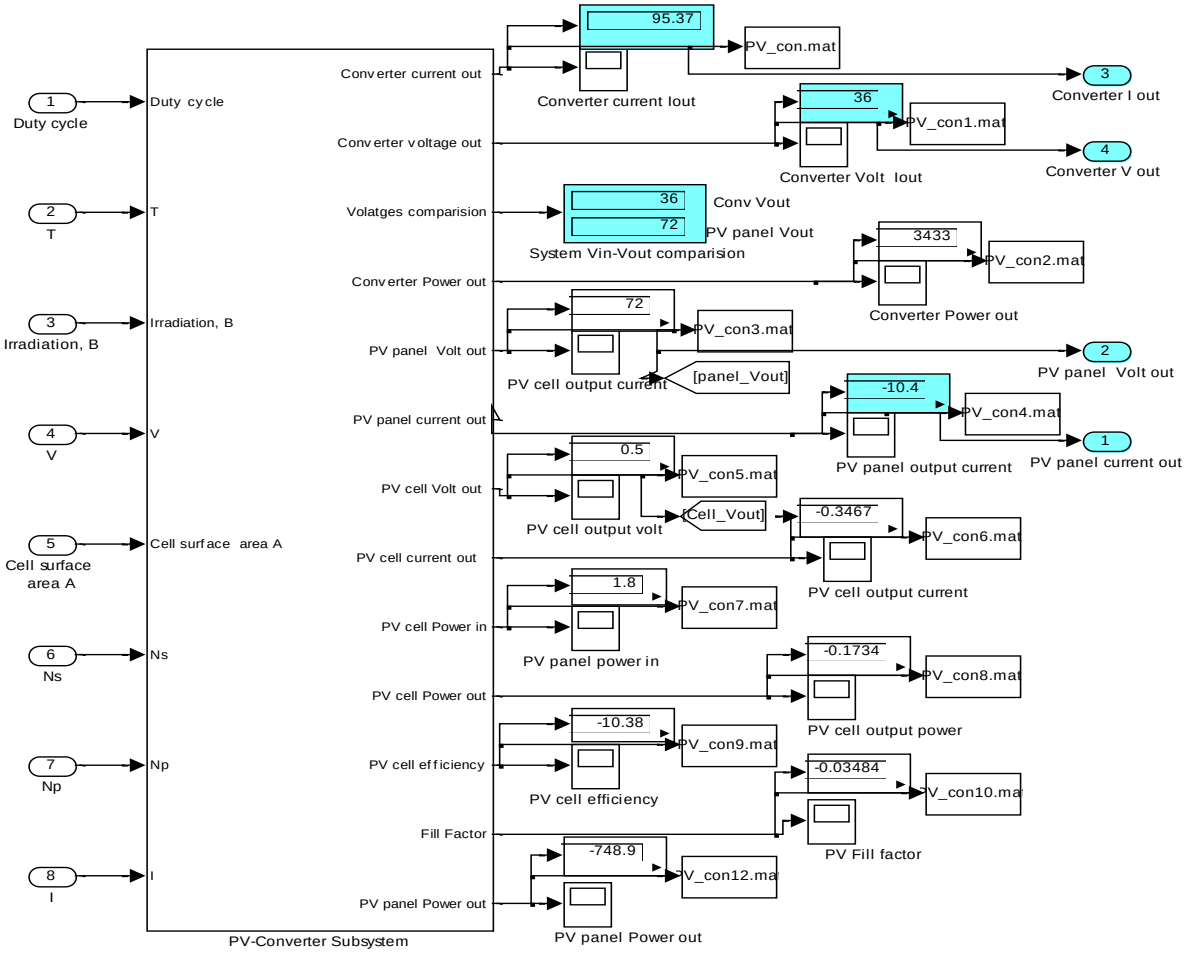

Figure 10(h) integrating PV panel sub-model and Converter sub-model in one mask sub-model

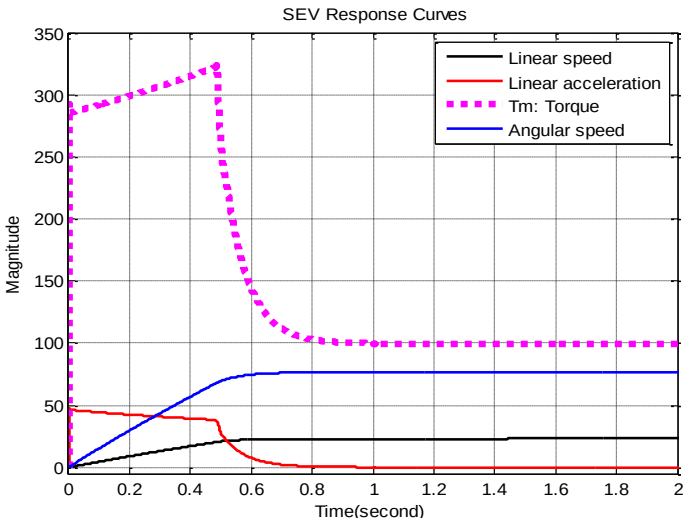

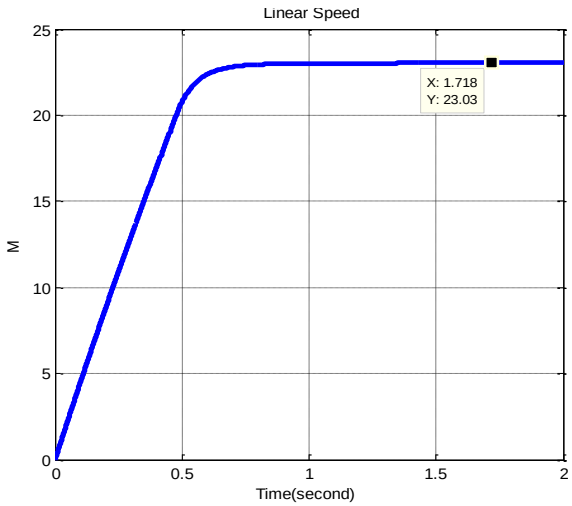

Figure 11(a) Linear speed, acceleration, current and motor torque Response curves of SEV

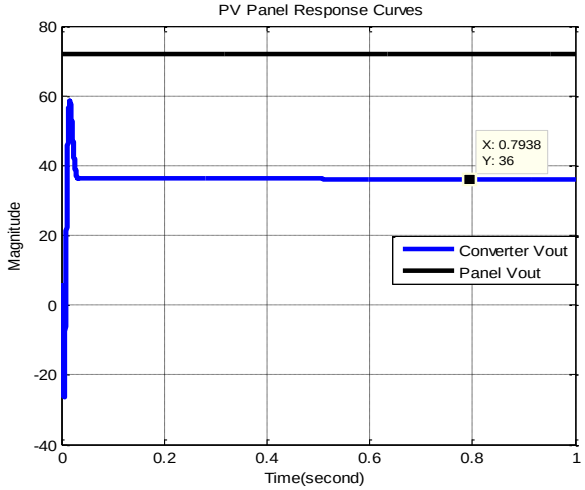

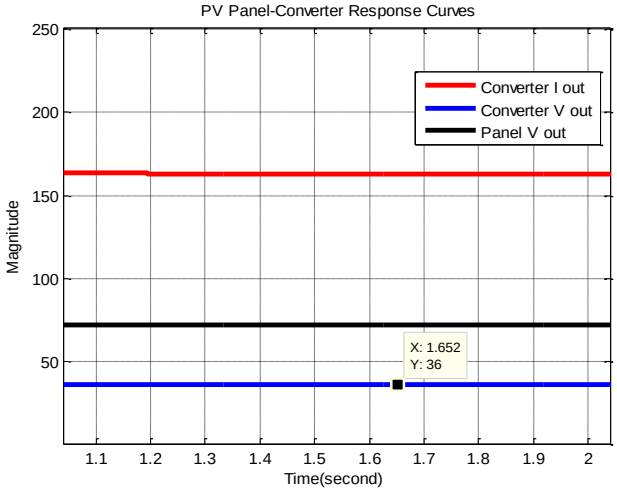

Figure 11(b) generated PV panel's output voltage and Converter's output voltage

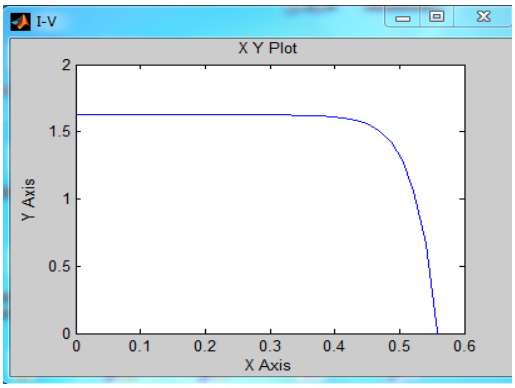

Figure 11(c) V-I Characteristics for β=200, and T=50

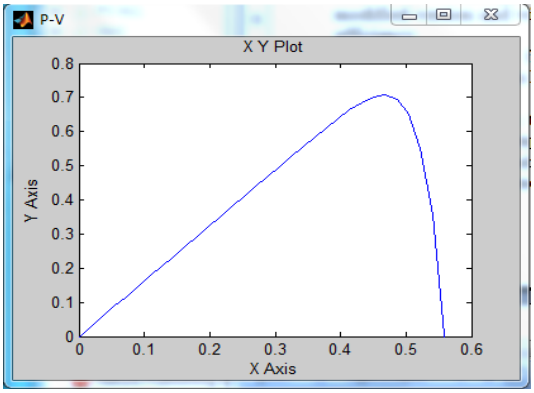

Figure 11(d) P-V Characteristics for β=200, and T=50

Table 1(a) Simulation results of each subsystem and whole SEDDMRP system for straight line motion

PVPC system inputs		**PV cell outputs**		**PV Panel outputs**		**Converter outputs**		**Both DC machines outputs**	
β	200	Voltage	0.5 V	Voltage	72 V	Voltage	36	Input voltage	36 V
T	75	Current	1.37 A	Current	41.01	Current	258.12	Max.Motor current	333.12 A
D	0.5	Fill factor	0.1374	Cell efficiency	1.277			Linear speed	23,2 m/s
A	0.0025	Power out	0.6835	FF	0.1374				
Ns	144	Power in	0.5						
Np	30	Efficiency	0.7315						

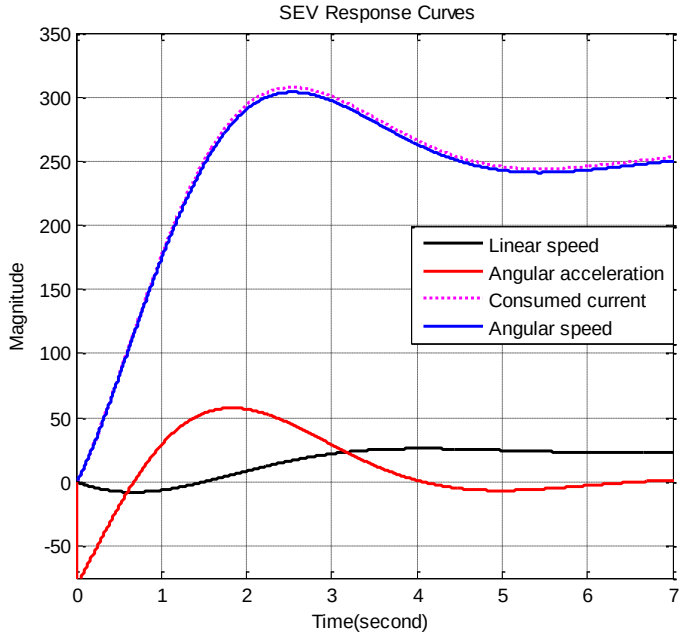

Figure 11(f) SEV responses to change in load torque

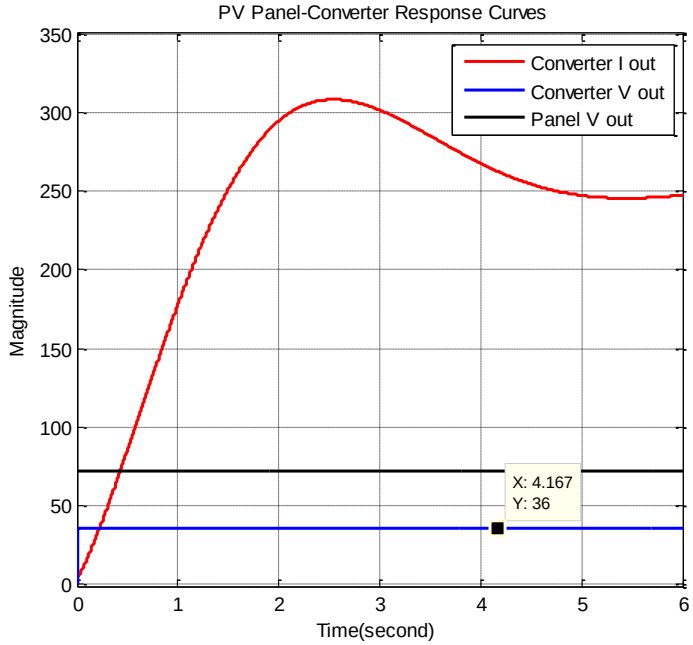

Figure 11(f) PV-panel converter outputs in response to change in load torque

Table 1 Nomenclature and nominal characteristic of SEV subsystems

DC machine parameters	
V_{in}=36 V	Input voltage to DC machine
K_t=1.188 Nm/A	Motor torque constant
R_a = 1 Ω	Motor armature Resistance
L_a=1 MH	Motor armature Inductance,
J_m=1.7 kg.m^2	Geared-Motor Inertia
b_m=1.1 N.m.s	Viscous damping
K_b=.985 rad/s/V	Back EMF constant,
n=1	Gear ratio
r=0.3 m,	Wheel radius
J_{equiv} kg.m^2	The total equivalent inertia,
b_{equiv} N.m.s	The total equivalent damping,
L=0.4 m	The distance between wheels centers
K_{tac}=0.4696rad/s	Tachometer constant,
ω=speed/r,	Angular speed rad/s
T_{shaft}	The torque produced by motor
η	The transmission efficiency
T_{shaft}	The torque, produced by the driving motor
Nominal values for SEV platform	
M,m, 1000 Kg	The mass of the mobile platform
C_d =0.75	Aerodynamic drag coefficient

C_L=0.01	The coefficient of lift, with values(C_L to be 0.10 or 0.16),
Cr=0.1	The rolling resistance coefficient
ρ , 1.25 *kg/m*^{3}	The air density at STP, ρ =1.25
a, m/s^2	Platform linear Acceleration
G, m/s^2	The gravity acceleration
N, m/s	The vehicle linear speed.
α , *Rad*	Road *slope* or the hill climbing angle
B	SEV platform's reference area
L	lift,
A_f	SEV frontal area
K_P	Proportional gain
K_I	Integral gain
Z_0	PI controller zero
P_m	The power available in the wheels of the vehicle.
T_{Total}	The total resistive torque, the torque of all acting forces.
	Solar cell parameters
Isc=8.13 A , 2.55 A , 3.8	The short-circuit current, at reference temp 25°C
I A	The output net current of PV cell (*the* PV *module current*)
I_{ph} *A*	The light-generated *photocurrent* at the nominal condition (25°C and 1000 W/m^2),
E_g *: =1.1*	The band gap energy of the semiconductor
$V_t = KT/q$	The thermo voltage of cell. For array :($V_t = N_s KT/q$)
I_s ,*A*	The reverse saturation current of the diode or leakage current of the diode
Rs=0.001 Ohm	The series resistors of the PV cell, it they may be neglected to simplify the analysis.
Rsh=1000 Ohm	The shunt resistors of the PV cell
V	The voltage across the diode, output
q=1.6e-19 C	The electron charge
B_o*=1000 W/m*^{2}	The Sun irradiation
β *=B=200 W/m*^{2}	The irradiation on the device surface
Ki=0.0017 A/◦C	The cell's short circuit current temperature coefficient
Vo= 30.6/50 V	Open circuit voltage
Ns= 48 , 36	Series connections of cells in the given photovoltaic module
Nm= 1 , 30	Parallel connections of cells in the given photovoltaic module
K=1.38e-23 J/oK;	The Boltzmann's constant
N=1.2	The diode ideality factor, takes the value between 1 and 2
T= 50 Kelvin	Working temperature of the *p-n* junction
T_{ref}*=273 Kelvin*	The nominal reference temperature

Buck converter parameters	
C=300e-6; 40e-6 F	Capacitance
L=225e-6 ; .64e-6 H	Inductance
Rl=RL=7e-3	Inductor series DC resistance
rc=	Capacitor equivalent series resistance,
RC=100e-3	ESR of C ,
V_{in}*= 24 V*	Input voltage
R=8.33; 5 Ohm;	Resistance
Ron=1e-3;	Transistor ON resistance
KD=D= 0.5, 0.2,	Duty cycle
Tt=0.1 , 0.005	Low pass Prefilter time constant
V_L	Voltage across inductor
I_C	Current across Capacitor

References

[1] Farhan A. Salem, Mechatronics Design of Small Electric Vehicles; Research and Education, International Journal of Mechanical & Mechatronics Engineering IJMME-IJENS Vol:13 No:01

[2] Bambang Sri Kaloko, Soebagio, Mauridhi Hery Purnomo, Design and Development of Small Electric Vehicle using MATLAB/Simulink, international Journal of Computer Applications (0975 – 8887) Volume 24– No.6, June 2011 .

[3] Dhameja, S., 2002, Electric Vehicle Battery Systems, Newnes, United Stated.

[4] Husain, I., 2003, Electric and Hybrid Vehicles Design Fundamentals, Pertama, CRC Press, United Stated.

[5] Larminie, J., Lowry, J. Electric Vehicle Technology Explained, John Wiley & Son , 2003.

[6] Tennessee valley authority at : http://www.tva.com/

[7] Ontario ministry of transportation, http://www.mto.gov.on.ca/english/

[8] Letendre S., Perez R., Herig C. (2003), Vehicle Integrated PV: A Clean and Secure Fuel for Hybrid Electric Vehicles, *Proc. of the American Solar Energy Society Solar 2003 Conference*, June 21-23, 2003, Austin,TX.

[9] Rizzo G. (2010), Automotive Applications of Solar Energy, 6th IFAC Symposium "Advances in Automotive Control", Munich, July 11-14, 2010..

[10] S.Letendre, R.Perez, Christy Herig, Vehicle Integrated PV: a Clean and Secure Fuel for Hybrid Electric Vehicles, *Proc. of Annual Meeting of the American Solar Energy Society, June 21-26, 2003, Austin, TX*.

[11] Ivan Arsie, Gianfranco Rizzo, Marco Sorrentino, OPTIMAL DESIGN AND DYNAMIC SIMULATION OF A HYBRID SOLAR VEHICLE, 2006-01- 2997SAE International.

[12] Hammad M., Khatib T. (1996), Energy Parameters of a Solar Car for Jordan, *Energy Conversion Management*, V.37, No.12.

[13] Wellington R.P. (1996), Model Solar Vehicles Provide Motivation for School Students, *Solar Energy* Vol.58, N.1-3.

[14] Seal M.R. (1995), Viking 23 - zero emissions in the city, range and performance on the freeway. *Northcon- Conference Record 1995. IEEE, RC-108*.p 264-268.

[15] Seal M.R., Campbell G. (1995), Ground-up hybrid vehicle program at the vehicle research institute. Electric and Hybrid Vehicles - Implementation of Technology *SAE Special Publications n 11051995*.SAE, Warrendale, PA, USA.p 59-65.

[16] Saitoh, T.; Hisada, T.; Gomi, C.; Maeda, C. (1992), Improvement of urban air pollution via solarassisted super energy efficient vehicle. *92 ASME JSES KSES Int Sol Energy Conf.* Publ by ASME, New York, NY, USA.p 571-577.

[17] Sasaki K., Yokota M., Nagayoshi H., Kamisako K. (1997), Evaluation of an Electric Motor and Gasoline Engine Hybrid Car Using Solar Cells, *Solar Energy Material and Solar Cells* (**47**), 1997.

[18] http://ww.itee.uq.edu.au/~serl/UltraCommuter.html

[19] Statistics for Road Transport, UK Government, http://www.statistics. gov.uk/ CCI/nscl. asp?ID=8100.

[20] Farhan A. Salem, Modeling and Simulation issues on Photovoltaic systems, for Mechatronics design of solar electric applications, IPASJ International Journal of Mechanical Engineering (IIJME), Volume 2, Issue 8, August 2014 .

[21] Farhan A. Salem, New generalized Photovoltaic Panel-Converter system model for Mechatronics design of solar electric applications,International Journal of Scientific & Engineering Research, Volume 5, Issue 8,August-2014 .

[22] Farhan A. Salem, Photovoltaic-Converter system, modeling and control issues for Mechatronics design of solar electric application, I.J. Intelligent Systems and Applications, 2014

[23] Farhan A. Salem, New generalized and refined Model for Mechatronics design of solar electric mobile robotic platforms,International Journal of Scientific & Engineering Research, Volume 5, Issue 8,August-2014 .

[24] Farhan A. Salem, Dynamic and Kinematic Models and Control for Differential Drive Mobile Robots, International Journal of Current Engineering and Technology , Vol.3, No.2, pp 253-263, June 2013.

[25] Farhan A. Salem, Mechatronics Design of Small Electric Vehicles; Research and Education, International Journal of Mechanical & Mechatronics Engineering IJMME-IJENS Vol:13 No:01, pp23-36, 2013.

[26] Farhan A. Salem, Modeling and control solutions for electric vehicle, European Scientific Journal edition vol.9, No.15,pp 221-240, May 2013

[27] Farhan A. Salem, Refined modeling and control for Mechatronics design of mobile robotic platforms. Estonian Journal of Engineering, 2013, 19, 3, 212–238.

[28] Farhan A. Salem, Modeling, simulation, controller selection and design of electric motor for Mechatronics motion control applications, using different control strategies and verification using MATLAB/Simulink, European Scientific Journal, September 2013 edition vol.9, No.27.

[29] Farhan A. Salem, Dynamic Modeling, Simulation and Control of Electric Machines for Mechatronics Applications, international Journal of control, automation and systems, Vol.1 No.2 , pp30-42,April 2013

[30] Farhan A. Salem, Modeling, Simulation and Dynamics Analysis Issues of Electric Motor, for Mechatronics Applications, Using Different Approaches and Verification by MATLAB/Simulink (I). I.J. Intelligent Systems and Applications, 2013, 05, 39-57.

[31] Farhan A. Salem, Mechatronics Design of Motion Systems; Modeling, Control and Verification , International Journal of Mechanical & Mechatronics Engineering IJMME-IJENS Vol:13 No:02, pp1-17, 2013.

[32] Ivan Arsie, Gianfranco Rizzo, Marco Sorrentino, Giovanni Petrone, Giovanni Spagnuolo, Mario Cacciato, Alfio Consoli, Hybrid Vehicles and Solar Energy: a Possible Marriage?, international conference on automotive technologies , ICAT Istanbul 2006.

[33] Gianfranco Rizzo, Ivan Arsie, Marco Sorrentino, Solar energy for cars: perspectives, opportunities and problems, GTAA Meeting, Mulhouse, 26-27 May, 2010.

[34] Farhan A. Salem , Mechatronics Design of Small Electric Vehicles; Research and Education, International Journal of Mechanical & Mechatronics Engineering IJMME-IJENS Vol:13 No:01, PP:23-36 , 2013.

[35] Brahim Gasbaoui, Abdelkader Chaker, Abdellah Laoufi, Boumediène Allaoua, Abdelfatah Nasri, The Efficiency of Direct Torque Control for Electric Vehicle Behavior Improvement , Sebian journal of electric engineering Vol. 8, No. 2, May 2011, 127-146.

[36] Daniel Fodorean, Global Design and Optimization of a Permanent Magnet Synchronous Machine Used for Light Electric Vehicle, *Technical University of Cluj-Napoca, Electrical Engineering Department Romania*.

[37] Qi Huang, Jian Li and Yong Chen, Control of Electric Vehicle, University of Electronic Science and Technology of China P.R.China.

[38] Massimo Barcaro , Nicola Bianchi , Freddy Magnussen, PM Motors for Hybrid Electric Vehicles, *The Open Fuels & Energy Science Journal*, 2009, *2*, 135-141 135.

[39] Parsa, L.; Goodarzi, A.; Toliyat, H. A. *Five-Phase Interior Permanent Magnet Motor for Hybrid Electric Vehicle Application*, Proceedings of the IEEE Vehicle Power and Propulsion Conference, VPPC'2005, Chicago: USA, 2005, pp. 631-637.

[40] Dutta, R.; Rahman, M. F. *Design and Analysis of an Interior Permanent Magnet (IPM) Machine with Very Wide Constant Power Operation Range*, Proceedings of the IEEE 32nd Annual Conference on Industrial Electronics, IECON'2006; Paris: France, 2006, pp. 1375-1380.

[41] Erik Schaltz, Electrical Vehicle Design and Modeling, InTech open access publishing, free online editions of InTech http://cdn.intechopen.com/pdfs/19571/InTech-Electrical_vehicle_design_and_modeling.pdf

[42] Farhan A. Salem, Dynamic Modeling, Simulation and Control of Electric Machines for Mechatronics Applications, international journal of control, automation and systems Vol.1 No.2, pp30-41, April, 2013.

[43] Ahmad A. Mahfouz, Mohammed M. K., Farhan A. Salem , Modeling, Simulation and Dynamics Analysis Issues of Electric Motor, for Mechatronics Applications, Using Different Approaches and Verification by MATLAB/Simulink (I). *I.J. Intelligent Systems and Applications,pp39-57* ,05, 39-572013

[44] Grzegorz SIEKLUCKI,Analysis of the Transfer-Function Models of Electric Drives with Controlled Voltage Source PRZEGL ˛ AD ELEKTROTECHNICZNY (Electrical Review), ISSN 0033-2097, R.88NR7a/2012.

[45] Zsuzsa Preitl, Péter Bauer, Cascade Control Solution for Traction Motor for Hybrid Electric Vehicles, Acta Polytechnica Hungarica, Vol. 4, No. 3, 2007.

[46] Farhan A. Salem, Mechatronics motion control design of electric machines for desired deadbeat response specifications, supported and verified by new MATLAB built-in function and Simulink model, European scientific journal vol. 9, No. 36 , December, 2013.

[47] Ahmad A. Mahfouz, Ayman A. Aly, Farhan A. Salem , Mechatronics Design of a Mobile Robot System, I.J. Intelligent Systems and Applications, 03, 23-36, 2013.

[48] Min Zhang , Modeling and Simulation of Hybrid Electric Vehicle Power Systems , *SAE TECHNICAL PAPER SERIES* , 2007-01-1592World CongressDetroit, Michigan,April 16-19, 2007

[49] Samer Alsadi, Basim Alsayid ,Maximum Power Point Tracking Simulation for Photovoltaic Systems Using Perturb and Observe Algorithm, International Journal of Engineering and Innovative Technology (IJEIT), Vol 2, Issue 6, pp80-85,December, 2012

Authors certify that there is no any conflict of interest (financial, personal or other relationships) that could inappropriately influence this work.

Authors Profile

Farhan Atallah Salem is currently with Taif University, Taif, Saudi Arabia. Dept. of Mechanical Engineering, Mechatronics Prog., College of Engineering, Email: salem_farh@yahoo.com

Ali S. Alosaimy is currently with Taif, University, Taif, Saudi Arabia., Dept. of Mechanical Engineering, Mechanical Power Engineering Prog. College of Engineering.